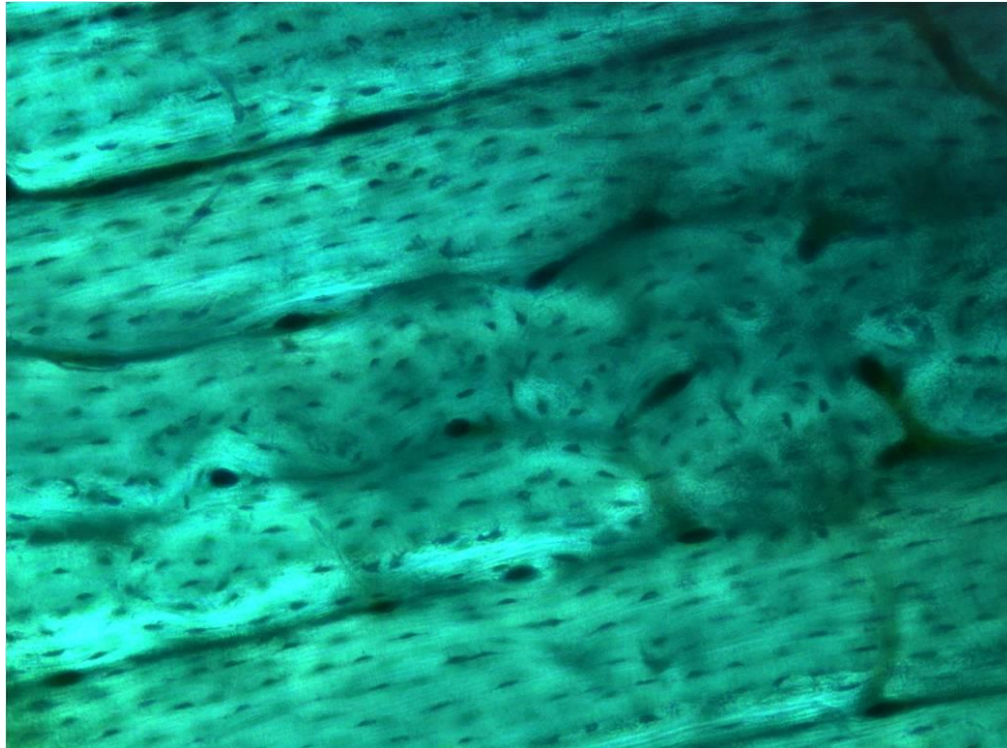


CHALMERS



The origin of lamellar structure in cortical bone

Master of Science Thesis in the Master Degree Program Biotechnology

Sara Bryngelsson Sprangers

Department of Applied Physics

Division of Biological Physics

CHALMERS UNIVERSITY OF TECHNOLOGY

Gothenburg, Sweden 2013/2014

The origin of lamellar structure in cortical bone

Sara Bryngelsson Sprangers

Cover image: A photo showing cow cortical bone with 10x magnification. The mineralized bone matrix is visualized in green while the cell nuclei can be seen as smaller black areas surrounding the Haversian canals.

"I agree with those African tribes who decorate themselves with bones. It is more to my taste than diamonds, which are a cold and soulless shine. Whilst bone, ah bone, is the pit of a man after the cumbering flesh has been eaten away. Bone is power. It is bone to which the soft parts cling, from which they are, helpless, strung and held aloft to the sun, lest man be but another slithering earth-noser . . . What is this tissue that has double the strength of oak? One cubic inch of which will stand a crushing force of two tons? This substance that refuses to dissolve in our body fluids, but remains intact and solid through all vicissitudes of temperature and pollution? We may be grateful for this insolubility, for it is what stands us tall."

—Richard Selzer, *Mortal Lessons*, Harcourt-Brace, San Diego, 1974, pp. 51–52

Abstract

Bone maturation is a highly complex process *in vivo* where several cellular events are still not completely understood. An example of this is the production of new unmineralized bone, or osteoid, by osteoblasts in cortical bone. The osteoid is subsequently mineralized into new bone in a step-wise process, which results in a structural appearance of layers of bone with different thickness. The theory investigated in this project is that the osteoblasts are guided in their osteoid production by the degree of mineralization of the secreted osteoid and that they preferably produce osteoid on a stiffer mineralized surface. To evaluate the influence of substrate stiffness on osteoblast development and osteoid production, pre-osteoblast MC3T3-E1 cells were cultured onto collagen type I - coated polyacrylamide (PA) substrates with stiffness 6.4 ± 0.7 kPa (soft), 72.9 ± 1.7 kPa (medium) and 135.9 ± 3.4 kPa (stiff). Type I collagen coated tissue culture polystyrene, with and without addition of 1,25-dihydroxyvitamin D₃ (1,25(OH)₂D₃), were applied as positive controls. Total cellular content of RNA and DNA for the MC3T3-E1 cells cultured onto the different substrates were determined, but no significant impact of substrate stiffness on the amount of total RNA and DNA could be detected after 48 hours of culture. The amount of total protein content for the MC3T3-E1 cells on the different substrates were too low to be detected. However, staining for alkaline phosphatase revealed a higher degree of differentiation among the MC3T3-E1 cells seeded onto the stiff substrate and plastic controls already after 24 hours. An up-regulation in gene expression of collagen type I, bone sialoprotein and osteopontin was further observed for the collagen coated plastic controls but no difference could be detected between the three sample substrates after 48 hours.

Osteoblasts experience a range of partly mineralized surfaces during the bone formation process *in vivo* and to mimic this pieces of cow bone were demineralized with EDTA for 6, 12, 24, 48 and 72 hours and further for 4, 7, 11, 14, 18 and 21 days. These were applied as alternative MC3T3-E1 cell substrates together with controls lacking demineralization. Staining to evaluate impacts of the demineralization treatment on seeded MC3T3-E1 cell after 48 hours revealed an increased degree of demineralization and presence of unmineralized flakes associated with prolonged EDTA treatment. Significant higher levels of total RNA and DNA were detected for the control bone pieces lacking demineralization compared to the bone pieces with demineralization but the protein levels were also in this case below the limit of detection. In general, stiffer substrates were shown to induce higher level of differentiation and proliferation among osteoblasts but no impact of substrate stiffness on metabolic activity could be identified. The substrate stiffness was shown to affect osteoblast maturation, with an accelerated process observed for the stiffer substrates, but more research is needed before any conclusions can be drawn considering the impact of substrate stiffness on osteoblasts during the formation of lamellar structure in cortical bone.

Acknowledgement

This master thesis project was performed at the Department of Cell Biology and Histology, Academisch Centrum Tandheelkunde Amsterdam (ACTA) in Amsterdam. A lot of people have been involved during the creation of this thesis and it would not have been possible without them. I cannot mention everyone by name but you all know that I am deeply thankful. There is however some people who deserves a specially acknowledgement. First of all I want to thank my two supervisors, Prof. dr Theo Smit and Ass. Prof. Astrid Bakker. This thesis would not have been possible without their continuous guidance and support! Second, my thesis examiner Assoc. Prof. Julie Gold is worth a special thanks for arranging everything practical with the examination process. It has been a privilege to work with all the wonderful people on the eleventh floor at ACTA in Amsterdam and I am very much looking forward to whatever comes next!

Abbreviation and explanation of important terms

Sections of this project contain words, abbreviations and expressions that need a brief introduction to facilitate the reading of the report.

Alizarin Red S	Staining used to detect the presence of calcium deposition by osteoblasts. It is commonly applied as a marker of matrix mineralization in <i>in vitro</i> bone research.
ALP	Alkaline phosphatase. An early marker of osteoblast differentiation.
Bone remodelling	Dynamic and lifelong process of reshaping and replacing bone tissue.
BMU	Basic Multicellular Unit. Where the bone remodelling process and formation of secondary osteons takes place.
Cortical bone	Compact structure of bone tissue.
Cancellous bone	Porous structure of bone tissue.
ECM	Extracellular matrix. Refers to the microenvironment outside the cell membrane.
EDTA	Ethylene diamine tetra-acetic acid. Applied in this project to demineralize bone pieces.
Goldner's trichrome staining	Three-colour staining technique used to visualize different parts of a histological sample. The colour dyes used are Weigert's Hematoxylin to stain cell nuclei black, Ponceau Acid Fuchin to stain unmineralized matrix red and Light green SF to stain mineralized tissue sections green.
Haversian canal	Central canal in circular osteons which provides the bone tissue cells with nutrients and oxygen.
Hydroxyapatite	Mineral which compose the major inorganic part of bone tissue.

Indentation	Technique to measure the mechanical properties of a sample with the use of a small probe.
Integrin	Trans-membrane receptors that mediate the attachment of a cell to the ECM.
Lamellar bone	The most abundant type of bone tissue, structured in lamellae of collagen type I.
MC3T3-E1 cells	A pre-osteoblast cell line derived from mouse.
Mechanotransduction	The conversion of mechanical stimuli into intracellular biochemical signals.
NBT/BCIP staining	Staining technique that detect ALP activity in a sample.
Osteoblasts	Bone cells responsible for the synthesis of new bone.
Osteocytes	Terminally differentiated osteoblasts embedded in their secreted bone matrix.
Osteoclasts	Multinucleated cells responsible for bone degradation.
Osteoid	The unmineralized bone matrix produced during the process of bone remodelling.
Polyacrylamide gel	Hydrogels commonly applied in research <i>in vitro</i> due to their tuneable mechanical properties.
RT-PCR	Reverse Transcription – Polymerase Chain Reaction. Technique to detect expression of one or several genes.
Sirius Red F3B	Staining technique used to detect presence of long extracellular fibers, such as collagen type I, in a sample.
Vitamin D	Enhancer of osteoblast differentiation and bone formation.
Wolff's law	States that bone is able to adapt its structure to the applied mechanical load.
Woven bone	The first bone created during growth or shortly after injury. The bone is produced fast and with disordered collagen type I fibres.

Contents

1. Introduction	1
1.1 Problem and hypothesis.....	2
1.2 Aim	2
1.3 Scope.....	2
2. Background	3
2.1 Bone architecture.....	3
2.1.1 Woven and lamellar structure	4
2.1.2 Cylindrical osteons.....	4
2.2 The lamellar structure within cylindrical osteons	5
2.2.1 Proposed model of the origin of lamellar structure.....	6
2.3 Four types of bone cells.....	7
2.3.1 Osteoblast	7
2.3.2 Bone lining cell	7
2.3.3 Osteocytes.....	7
2.3.4 Osteoclasts.....	7
2.4 Substrate stiffness affect cell development and behaviour	8
2.5 The process of bone remodelling	9
2.6 Valid bone formation markers.....	10
2.6.1 Bone sialoprotein	10
2.6.2 Collagen type I.....	10
2.6.3 Alkaline phosphatase.....	10
2.6.4 Osteocalcin	10
2.6.5 Osteopontin.....	10
2.7 Culture and maintenance of MC3T3-E1 cells.....	11
2.7.1 Vitamin D induces MC3T3-E1 differentiation.....	11
2.8 Techniques for development of substrates with different stiffness	12
2.8.1 PA gels with pre-determined stiffness.....	12
2.8.2 Demineralized cow bone	13
2.9 Analytical techniques	14
2.9.1 Nanoindentation	14
2.9.2 Reverse Transcription – Polymerase Chain Reaction	15

2.9.3	NBT/BCIP staining.....	15
2.9.4	Sirius Red F3B staining	15
2.9.5	Goldner's trichrome staining.....	16
2.9.6	Alizarin Red S staining.....	16
2.10	Choice of substrate stiffness and culture time.....	17
3.	Materials and methods.....	18
3.1	MC3T3-E1 culture maintenance	18
3.2	Preparation of MC3T3-E1 substrates	18
3.2.1	Cow bone demineralization with EDTA.....	18
3.2.2	Fabrication and functionalization of PA gels	18
3.2.3	Fabrication and functionalization of plastic control substrates	20
3.2.4	Determined stiffnesses of the PA gels.....	20
3.3	MC3T3-E1 cell experiments.....	21
3.4	Gene expression of valid bone formation markers.....	21
3.4.1	Isolation of RNA	21
3.4.2	Isolation of DNA	22
3.4.3	Isolation of proteins	22
3.4.4	Detection of gene expression of bone formation markers	23
3.5	Detection of ALP activity.....	23
3.6	Staining with Sirius Red F3B.....	23
3.7	Staining with Alizarin Red S.....	23
3.8	Staining with Goldner's trichrome.....	24
3.9	Statistical analysis.....	24
4.	Results.....	25
4.1	Stiffness of the PA gels used.....	25
4.2	Substrate stiffness dictate osteoblast morphology	26
4.3	Osteoblast proliferation on substrates with various stiffness.....	27
4.4	Osteoblast differentiation on substrates with various stiffness.....	29
4.5	Gene expression of bone formation markers	31
4.6	Impact of substrate stiffness on osteoblast metabolic activity	32
4.7	Matrix mineralization induced by substrate stiffness	33
4.8	Demineralization of bone pieces.....	34
4.9	Osteoblast proliferation on partly demineralized bone.....	36

5. Discussion	38
5.1 Choice of substrates	38
5.2 Effect of substrate stiffness on osteoblast activity	40
5.3 Substrate stiffness guide osteoblast differentiation	42
5.4 Impact of substrate stiffness on osteoblast gene expression	42
5.5 Osteoblast induced mineralization of ECM	43
6. Conclusions.....	45
7. Future prospective	46
8. References.....	47
Appendix A.....	51
A.1 MC3T3-E1 medium, passaging and seeding	51
A.2 Process of bone demineralization	53
A.3 Production of polyacrylamide (PA) gel substrates	54
A.4 Application of coating.....	55
A.5 Experiments with PA gel substrates	57
A.6 Experiments with demineralised bone substrates	59
A.7 Isolation of RNA, DNA and proteins	60
A.8 Detection of bone formation markers with RT-PCR.....	63
A.9 Staining with NBT/BCIP	65
A.10 Staining with Sirius Red F3B.....	66
A.11 Staining with Alizarin Red S.....	67
A.12 Staining with Goldner's trichrome.....	68
Appendix B	70
List of used materials.....	70

1. Introduction

Bone is a rigid yet dynamic tissue which throughout life is able to grow, adapt its structure, self-repair when fractured and continuously renew itself by internal bone remodelling. During this life-long remodelling process of the skeleton an osseous tissue type known as cortical bone is formed. This is the strongest and most abundant structure type of adult human bone and its dense appearance is crucial for several functions associated with the skeleton, such as support, organ protection and mineral storage and deposition. The creation of cortical bone during the remodelling process of the skeleton includes among others bone degrading osteoclasts and bone producing osteoblasts. These specialized bone cells work in a coordinated fashion within spatial organizations known as bone multicellular units (BMUs) to create a structure consistent of several collagen type I layers with thickness ranging from 3 to 7 μm [1]. This architecture is frequently referred to as lamellar and is a result of a discontinuous process where osteoblasts step-wise produce an unmineralized collagen matrix, or osteoid, which subsequently is mineralized into new bone.

The importance of ECM stiffness to steer the fate of attached cells has been well documented in later years and nearly all cell types have been proven to be mechanosensitive, *i.e.* they adapt in response to biophysical factors of the ECM [2]. The mechanosensing mechanisms in bone cells are still poorly understood and the complex mechanical environment to which bone cells are exposed complicates the separation of specific effects of ECM stiffness from the influence of strain, fluid shear stress, pressure *etc.* It is however clear that several, if not all, of these biophysical parameters have the ability to independently regulate responses in bone cells and stiffer substrates have repeatedly been observed to induce differentiation in the direction of the osteoblast lineage [3]. During the production of lamellar structure in cortical bone the osteoblasts experience a broad range of ECM stiffness when the secreted bone matrix gradually is mineralized into new hard bone. A certain amount of newly produced bone matrix offers a soft substrate and a completely different set of mechanical signals to the osteoblasts as compared to partly or completely mineralized bone matrix. The mechanical properties of the lamellar structure in mature cortical bone have been widely studied in recent years [1][4] but the effect of this gradually change in substrate stiffness on the action of osteoblasts during the production of lamellar structure in cortical bone remains elusive. Even though the interaction between bone cells and their mechanical environment *in vivo* is complex, a more extensive understanding of the influence of mechanical regulation from ECM stiffness during the remodelling process of cortical bone is crucial. A deeper knowledge of cellular processes in bone contributes to a more comprehensive understanding of bone physiology and ultimately in the development of more refined methods to improve skeleton therapies.

1.1 Problem and hypothesis

Even though the structure of lamellar bone is long known and amply described in literature, the underlying mechanisms and cellular processes which guide the osteoblasts in its step-wise secretion remains unknown. The working theory in this project is that osteoblasts are activated and stimulated to produce bone matrix when a certain degree of osteoid mineralization has been achieved and they sense a stiffer bone surface. The osteoblasts will produce and secrete osteoid until they receive a new cascade of signals from the softer matrix and stop producing new osteoid until enough mineralization of the matrix has been achieved. When the osteoblasts once again sense a stiffer bone surface they resume the osteoid production, which results in the distinct lamellar structure in cortical bone.

1.2 Aim

The principal aim of this project is to evaluate the possibility that osteoblasts are guided in their osteoid production in response to the altered stiffness of the local ECM during the mineralization process. The hypothesis will be investigated by seeding pre-osteoblast MC3T3-E1 cells onto hydrogels with different Young's modulus and pieces of partly demineralized bone. The impact of substrate stiffness on different aspects of osteoblast development will be investigated with both quantitative and qualitative experimental analysis *in vitro* to obtain an indication of the impact of ECM stiffness on osteoblast osteoid production *in vivo*.

1.3 Scope

The limited time span of this master thesis project results in the following restrictions:

- Only three different stiffnesses will be used to evaluate the impact of substrate stiffness on osteoblast development.
- The nature of the mechanical signals induced by the stiffness of the substrates will not be analysed.

2. Background

2.1 Bone architecture

Bone tissue is a highly optimized and complex material with an universal arrangement that varies only slightly with specie, age and sex. Bone is mainly composed of collagen type I fibrils together with the mineral hydroxyapatite [HA, $\text{Ca}_{10}(\text{PO}_4)_6(\text{OH})_2$] and due to the variety of mechanical loadings of bone the structural arrangement of these two components is crucial. The collagen fibrils are organized in helical fibres, between which the minerals are incorporated, as seen in Figure 1.

From a macroscopic point of view there are two distinct bone structures that significantly contribute to the structural strength of the skeletal system: cortical (compact) bone and cancellous (spongy) bone. The latter one is highly porous and its interconnected pores are filled with bone marrow containing blood vessels, nerves and a variety of different cell types. The cortical bone on the other hand is denser and forms the rigid and uniform external shell surrounding the cancellous bone [5]. This arrangement of cancellous and cortical bone result in a structure assumed to be optimized for a broad range of mechanical loads [6].

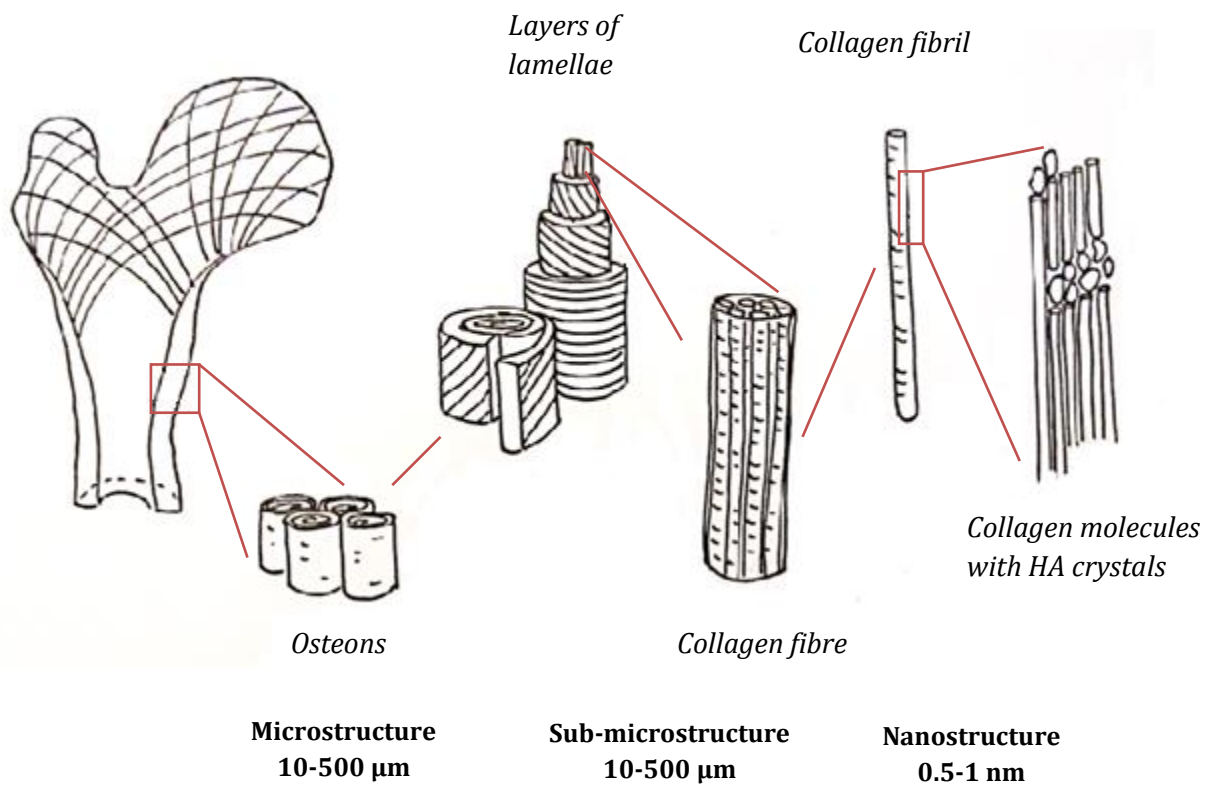


Figure 1. The hierarchical structure of cortical bone from macro- to nanostructure.

2.1.1 Woven and lamellar structure

Microscopically two types of bone can be identified within cortical bone. Woven bone is created at a high rate *de novo* on top of already existing bone surface during skeletal growth or shortly after a fracture [7]. It is an immature and mechanically weak bone structure with an disordered organization of the collagen fibres. The second bone structure is lamellar bone, which has a regular organization of the collagen fibres and is mechanically strong due to the presence of stable cylindrical osteons [8], as seen in Figure 2. Lamellar bone therefore usually replaces woven bone by time and is the most abundant bone tissue type in mammals.

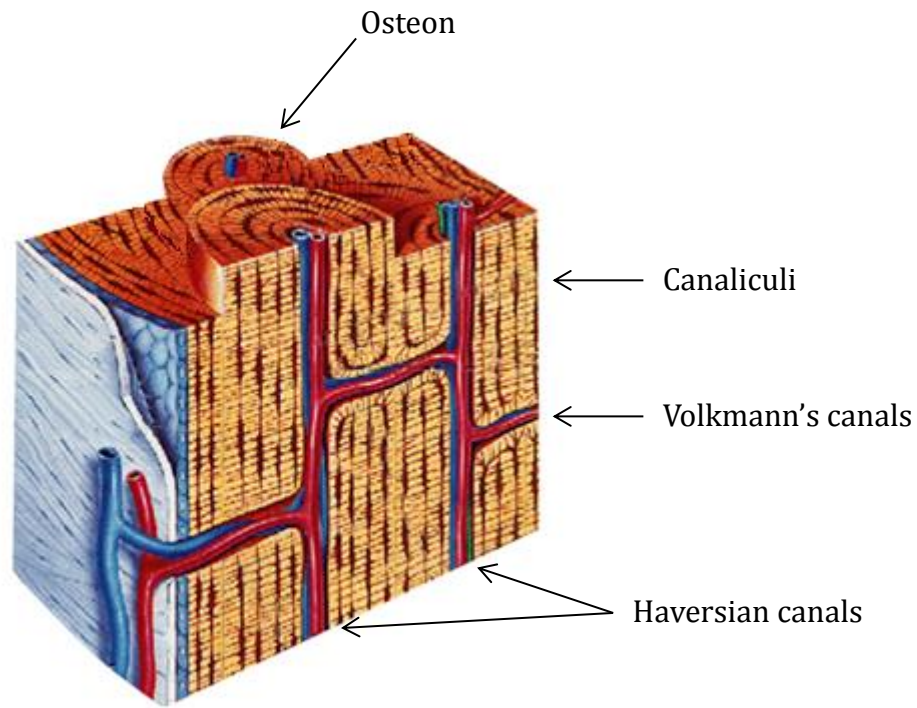


Figure 2. Cross-section of cylindrical osteons with central Haversian canals, transverse Volkmann's canals and the interconnecting canaliculi. Figure adapted from "The Toughness of Bone", Berkeley Lab News Center (2008).

2.1.2 Cylindrical osteons

Cylindrical osteons are also known as Haversian systems after the English physician Clopton Havers (1657-1702), who was the first to describe their existence [9]. These osteons contain blood vessels and nerves in a central cavity, usually referred to as the Haversian canal, which provides the inner tissue of the bone with nutrients and oxygen. Several smaller canals known as canaliculi ("little canals") radiate out from the Haversian canal and others, referred to as Volkmann's canals, runs perpendicular to the central cavity and connect the different canals with one another and to the outside surface of the bone.

2.2 The lamellar structure within cylindrical osteons

Even though lamellar bone is the most abundant type of bone structure in mammals its appearance remains a subject of controversy [10]. The reason for debate is the nature of the distinct collagen layers, or bone lamellae, surrounding the Haversian canal in the cylindrical osteons. Two main theories explaining the appearance of this lamellar have been proposed and won advocates during the decades. The first one consider the lamellar structure a result of a slight rotation of the collagen type I fibrils for succeeding layers lamellae while the second instead suggests that the lamellar pattern is due to alternating rich and poor layers of collagen type I, creating layers of dense and loose lamellae respectively [10]. The former is known as Gebhardt's model and currently the one that is accepted by the majority of researchers. In 1988, this structural model was further refined and described as "twisted plywood" by the Giraud-Guille research group Using transmission electron microscopy (TEM) Weiner *et al.* further suggested in 1997 that each lamellar unit in the twisted plywood model is consistent of five arrays of parallel collagen fibres with a rotation of 30° compared to the succeeding lamellar unit [12], [11]. A schematic picture of the twisted plywood model is presented in Figure 3A-C.

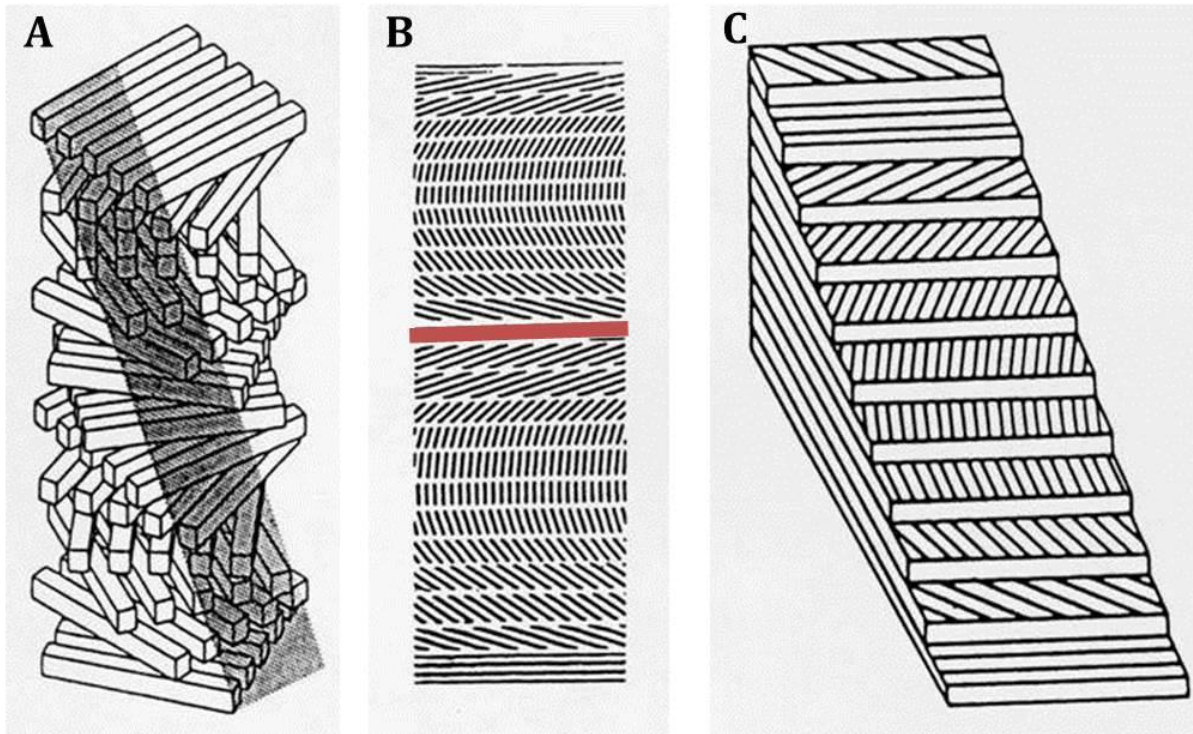


Figure 3. Schematic pictures of the twisted plywood model. (A) The five parallel collagen fibres with 30° rotation of the first lamellar unit compared to the succeeding. (B) The twisted plywood pattern visualized in a longitudinal section of an osteon, with the central Haversian canal in red and the resulting lamellar structure with rotated collagen fibres. (C) The resulting lamellar of twisted collagen fibres giving rise to the name "twisted plywood" model. Figure adapted from "Skeletal Tissue Mechanics", Martin, R. *et al.* (1998).

The second hypothesis has fewer advocates than the twisted plywood model. However, based on early research performed by Ruth in 1947 [13], Marotti *et al.* studied the same lamellae in different sections using scanning electron microscopy [14]. This revealed the presence of the proposed collagen rich and collagen poor layers, with bone cells only discovered in the loose lamellar. The same study further suggested that previous studies, suggesting the twisted plywood model, was based on photos taken at a too high magnification and that what they interpreted as a single lamellae instead was bundles of collagen fibres within a lamellae. Most investigators still support the idea that the twisted plywood model provide the best explanation for the lamellae pattern in cylindrical osteons [15] [16] [17], but both of the proposed theories have gradually recruited followers and conflicting observations still remain.

2.2.1 Proposed model of the origin of lamellar structure

Not much is known about its origin of the lamellar pattern in cylindrical osteons and the model which currently have most advocate was proposed by Marotti in 1993 [18]. This theory suggests that the lamellar structure is the result of interrupted contact between the bone cells osteoblasts (see section 2.3.1) and osteocytes (see section 2.3.3). The osteocytes elongate vascular dendrites during bone formation in order to remain in contact with the progressing osteoblasts. When the osteocytes cannot elongate their dendrites any further the contact between osteocytes and osteoblasts decrease, which in turn is believed to induce differentiation of the osteoblasts into stationary osteocytes, and a new lamellae is created when the process continue with the new osteocyte. Later studies have however been able to neither support nor contradict this theory due to practical difficulties with experimental setup *ex vivo*.

2.3 Four types of bone cells

There are four cells types present in bone tissue. The osteoblast, bone lining cell and osteocyte are of mesenchymal stem cell origin, while the osteoclast belongs to the macrophage family. They all play important and distinguished roles in maintenance and remodelling of bone, and they are briefly introduced below.

2.3.1 Osteoblast

Osteoblasts are cells that mainly are responsible for the production of new bone tissue. They are specialized and terminally differentiated bone cells originating from mesenchymal stem cells. Activated osteoblasts synthesize unmineralized bone matrix, or osteoid, which is their only specific morphological feature ^[19]. Single osteoblasts cannot produce osteoid and they operate therefore never in isolation or small groups, but rather in colonies with extensive contact between individual osteoblasts.

2.3.2 Bone lining cell

Subsequently the osteoblasts “retires” at the bone surface as flat and elongated bone line cells. These cells have a flattened morphology and clean pits created during bone resorption in order to facilitate for osteoblasts to deposit new osteoid ^[20]. The bone lining cells are relatively inactive forms of osteoblasts and little is known about their precise role. It is however generally accepted that they constitutes a functional protective layer of the bone surface and are important for the maintenance of bone fluids ^[21].

2.3.3 Osteocytes

A fraction of the osteoblasts becomes entombed within the newly produced osteoid and remain in the mineralized bone matrix as osteocytes. This is the most abundant cell type found in bone tissue ^[22] and their main function is to act as stationary regulators of the bone remodelling process in response to different stimuli. The osteocytes are characterized by their long, cytoplasmic extensions and dendrite-like morphology. With these extensions the osteocytes can communicate with each other and its adjacent environment through the extensive canaliculi network.

2.3.4 Osteoclasts

Osteoclasts are large multinucleated cells which initiate the bone remodelling process by the degradation of selected bone tissue with the release of a cocktail of resorbing enzymes. Unlike the other bone cells, which have the common origin from mesenchymal stem cells, osteoclasts have a different origin due to fusion in the bone marrow of mononuclear progenitors of the macrophage family ^[23]. During the initiation of the bone resorption process, the osteoclasts attach to the bone and form a specialized cell membrane known as the “ruffled border”, which increase the osteoclast cell surface and facilitates bone degradation.

2.4 Substrate stiffness affect cell development and behaviour

In the late 19th century the German surgeon Julius Wolff observed that bone adapts in order to optimize its load bearing capacity, which later became referred to as “Wolff’s law”. Today it is known that the mechanical properties of the microenvironment is crucial for accurate cell development and have a profound effect on cellular morphology and protein expression [3]. The local stiffness of the ECM is transmitted into intracellular signalling pathways, in a process known as mechanotransduction, and can guide the differentiation of mesenchymal stem cell (MSC) into a variety of different cell types. Soft substrates which mimic brain tissue have been proven neurogenic [24], stiffer substrates that resemble muscle tissue are myogenic [25] and even more rigid substrates similar to collagenous bone tissue are osteogenic [26] [27] [28].

The process of mechanotransduction within osteoblasts is complex with several receptors sensitive for mechanical stimuli involved. These receptors are often referred to as mechanotransducers or mechanosensors, where integrins is one of the most studied in osteoblast biology [29]. Binding of integrins to the ECM is performed via focal adhesions connected to the cytoskeleton, as seen in Figure 4. The ability of a stiff substrate to resist deformation induce stable focal adhesion, a more extensive cytoskeleton and a more elongated morphology of the attached osteoblasts [30]. Upon stimulation of the mechanosensors a cascade of enzymes are released. Further are MAPKs, Cox-2, NO, TNF- α and Wnt- β -catenin activated and growth factors, such as IGF, VEGF, PDGF, bFGF, TGF- β and BMP, secreted. The activation of intracellular signalling pathways and secretion of growth factors stimulate Runx2, which is the principal transcription factor for osteoblast differentiation [31] [29].

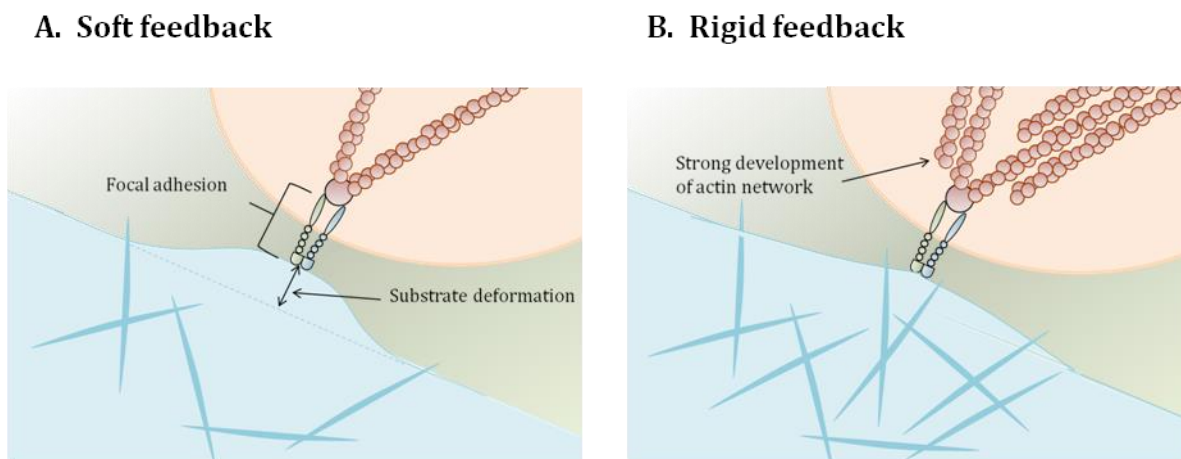


Figure 4. Schematic picture showing cellular response to substrates of different stiffness. (A) Substrate with low bulk stiffness have a greater distance between collagen fibres, which is sensed by cells as low resistance to the forces they exert via mechanosensors. Deformation of the bulk appears and the cells fail to assemble a strong actin cytoskeleton. (B) Substrate with high bulk stiffness offers rigid feedback to the cells when force is applied, which ultimately results in actin polymerization and a more developed cytoskeleton.

2.5 The process of bone remodelling

Bone is able to adapt to a range of different mechanical loads but repeated wear creates microdamages which subsequently would cause fractures if the skeleton was not constantly remodelled. This is done by bone cells arranged within temporary anatomical structures known as Bone Multicellular Units (BMUs), as seen in Figure 5. The BMU is comprised of a cutting cone and a closing cone, with a resting zone separating them. The osteoclasts (see section 2.3.4) are located at the tip of the cutting cone and lead the remodelling procession by excavating the bone. The osteoblasts (see section 2.3.1) are located in the closing cone of the BMU, filling the cavity with new osteoid composed of collagen and proteoglycans and direct its mineralization. Details concerning the intercellular signalling within the BMU is not completely understood but the embedded osteocytes (see section 2.3.3) are thought to guide the process through their interconnected network [32].

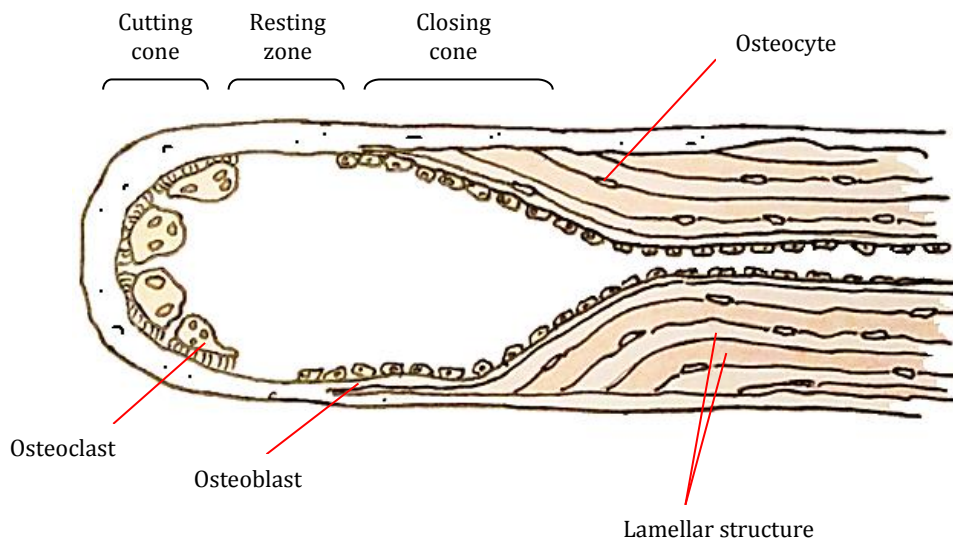


Figure 5. The Bone Multicellular Unit (BMU) where the bone remodelling process is taken place. The BMU include osteoclasts, located in the cutting cone, osteoblasts in the closing cone and embedded osteocytes.

Not much is known about how sites of bone remodelling is selected but since the process is initiated at previously quiescent surfaces it is assumed to be monitored by osteocytes and bone lining cells (see section 2.3.2) [33]. Osteocytes and bone lining cells have been proposed to identify the need of remodelling at a specific bone location based on a change in mechanical signalling or released molecules from the interior of the bone tissue [34]. The osteocytes and bone lining cells further recruit circulating osteoclasts, which remove the hydroxyapatite crystals from the calcified bone matrix with acid and degrade the remaining collagen fibrils with several specialized enzymes [35]. Stimulated by these and other factors released from the degraded bone [36] the mature osteoblasts secrete osteoid which ultimately forms the new bone.

2.6 Valid bone formation markers

Bone Turnover Markers (BTMs) are direct or indirect products generated by mature osteoblasts during the process of bone remodelling. Five commonly used osteoblast markers are briefly introduced below together with their primers presented in Table 1. The primer sequences for the markers presented.

2.6.1 Bone sialoprotein

Bone sialoprotein (BSP) is one of the major non-collagenous components of the bone matrix and has a documented enhancing effect on proliferation, differentiation and mineralization of osteoblasts [37]. The expression of the protein has been proposed to initiate hydroxyapatite formation during the mineralization process [38].

2.6.2 Collagen type I

Collagen type I is by far the most abundant organic component of the bone matrix, comprising about 90% of the bone matrix [39]. It is expressed early in osteoblast development is therefore a commonly used marker of bone formation.

2.6.3 Alkaline phosphatase

Bone specific alkaline phosphatase (BALP) is a marker for mature osteoblasts [40]. Its mode of action is not completely known but it is believed to be required to initiate osteoid mineralization.

2.6.4 Osteocalcin

Osteocalcin is a late stage marker of osteoblast differentiation and the most abundant non-collagenous protein in the extracellular bone matrix [19]. It is a widely used marker for osteoblast differentiation and is closely association with matrix mineralization [40].

2.6.5 Osteopontin

Osteopontin belongs to the same protein family as bone sialoprotein and has a wide spectrum of biological activities. It is expressed during both early and late osteoblast development and has been reported to play a key role in the adaptive response of the skeleton [41].

Table 1. The primer sequences for the markers presented.

Bone marker	Gene name	Forward primer	Reverse primer
BSP	<i>Bsp</i>	AACAATCCGTGCCACTCA	GGAGGGGGCTTCACTGAT
Collagen type I	<i>Col1a1</i>	GAGGCATAAAGGGTCATCGTGG	CATTAGGCGCAGGAAGGTCAGC
ALP	<i>Alpl</i>	GGGGACATGCAGTATGAGTT	GGCCTGGTAGTTGTTGTGAG
Osteocalcin	<i>Ocn</i>	CTGGCCCTGGCTGCGCTCTGT	GGTCCTAAATAGTGATACCGTAGATGC
Osteopontin	<i>Opn</i>	CTGCTAGTACACAAGCAGACA	CATGAGAAATTCGGAATTTTCAG

2.7 Culture and maintenance of MC3T3-E1 cells

The MC3T3-E1 is established as an immortalized pre-osteoblast cell line derived from mouse calvarium tissue, which is able to differentiate into mature osteoblasts *in vitro* and mineralize its surrounding matrix in culture. The developmental process of MC3T3-E1 cell cultures is characterized by an initiation phase of 1-2 weeks during which the cells slowly proliferate, express bone-specific genes and secrete osteoid [42] [37]. During the succeeding maturation phase after about 2 weeks, mineralization of the secreted matrix can be expected to occur [43].

Animal osteoblast models like MC3T3-E1 cells do not represent the human bone biology as accurate as primary cultures of human osteoblasts but they typically proliferate faster and experimental analysis is more readily conducted [44]. The primary human osteoblasts also have a tendency to stop proliferating before reaching confluence, thus greatly limiting the possibilities of obtain sufficient cell numbers for various experimental conditions.

2.7.1 Vitamin D induces MC3T3-E1 differentiation

Vitamin D is essential for bone mineralization and a commonly applied inducer of osteoblast differentiation *in vitro* [45] [46]. It has been shown that vitamin D increase ALP activity and matrix mineralization as well as alter the synthesis of bone matrix proteins, such as collagen type I and osteocalcin [43]. The most active form of vitamin D is thought to be 1,25-dihydroxyvitamin D₃ (1,25(OH)₂D₃), which represses or enhances the expression of several key parameters during bone turnover [47]. The specific binding of vitamin D to a receptor located in the cell membrane stimulates genomic responses and cellular responses are also mediated via non-specific receptors. However, despite the numerous actions of vitamin D not much is known about the mechanism by which it stimulates bone mass and how this effect is impacted by other bone regulating factors, such as mechanotransduction [45].

2.8 Techniques for development of substrates with different stiffness

Polyacrylamide (PA) gel is a form of hydrogel which is commonly applied as cell substrate *in vitro* due to its tuneable mechanical properties. Partly demineralized bone pieces have more fixed mechanical properties but are applied as osteoblast substrate to obtain a more accurate mimic of the *in vivo* bone environment.

2.8.1 PA gels with pre-determined stiffness

Polyacrylamide (PA) gels are chemically inert hydrogels composed of a network of loosely organized fibres. The mechanical properties of PA gels can be widely tuned by changing the mixing ratio of its two main components: acrylamide and bis-acrylamide. The polymerization reaction is initiated by the addition of tetramethylethylenediamide (TEMED), which reacts with added ammonium persulfate (APS) and accelerates the formation of free radicals. These highly reactive compounds further converts the acrylamide monomers into free radicals which react with inactive acrylamide monomers and initiate the polymerization process. The elongating acrylamide polymers are randomly crosslinked with bis-acrylamide to form polyacrylamide [48], as seen in Figure 6. The resulting PA gel is characterized by mechanical stiffness dependent on polymerization conditions and concentration of acrylamide and bis-acrylamide. Increased initial monomer concentrations results in more crosslinks between acrylamide and bis-acrylamide and an increased stiffness of the produced PA gel.

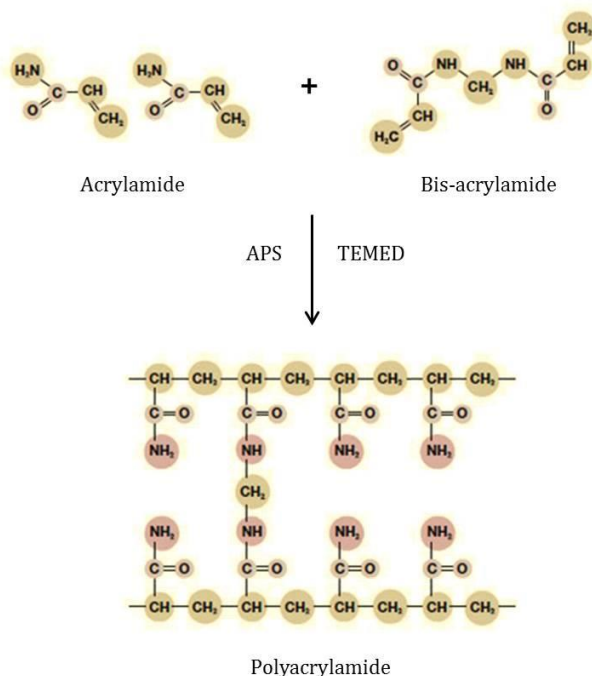


Figure 6. The crosslinking between acrylamide and bisacrylamide, via addition of ammonium persulfate (APS) and tetramethylethylenediamide (TEMED), forms polyacrylamide.

The PA gels allow production of a wide range of defined and reproducible stiffnesses, thus providing an efficient way to investigate the impact of substrate stiffness on osteoblast behaviour. Since the PA gels do not naturally support cell attachment they were coated with collagen type I prior to cell seeding.

2.8.2 Demineralized cow bone

Different stiffness of bone can be obtained via bone demineralization with treatment of HCl or ethylene diamine tetra-acetic acid (EDTA) solutions. With longer demineralization time more minerals are removed and the remaining bone tissue becomes softer and more elastic. However, while HCl destroys the collagen structure of bone by inducing hydrolysis of the fibres, bone demineralization by EDTA results in an almost completely preserved collagen type I structure and DNA content [50]. This is due to the fact that the EDTA both demineralises the bone and inactivates DNAses by chelating agents, such as Mg^{2+} and Ca^{2+} [51].

2.9 Analytical techniques

Several techniques are available to evaluate the impact of substrate stiffness on different aspects of osteoblast proliferation, gene expression, differentiation, metabolism and matrix crystallization. The techniques applied in this project are briefly presented below.

2.9.1 Nanoindentation

Instrumented nanoindentation is a frequently applied method to characterize the mechanical stiffness of materials with low values of Young's modulus. In general, a hard probe with known properties is pressed into the material with unknown properties, as seen in Figure 7. An increased force is applied via an indenter with an exchangeable probe onto the sample material, resulting in a plastic deformation of the material. The area and depth of this material impression is a direct result of the properties of the probe and the applied force, which is monitored by constant signal feedback from the indenter and its two attached springs. The springs are chosen based on the assumed stiffness of the substrate in order to obtain a measurable deformation of the material of interest [52].

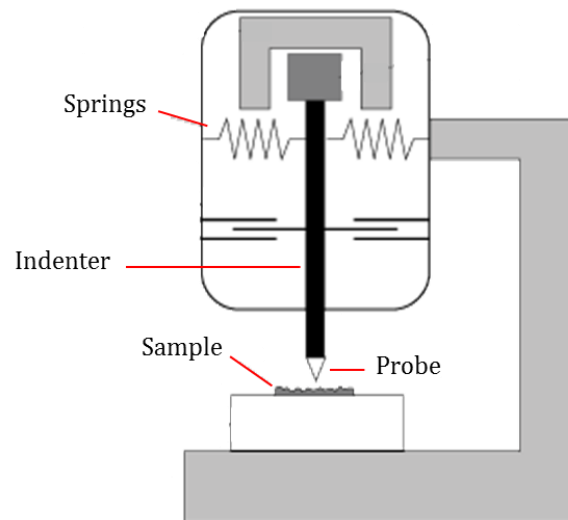


Figure 7. A schematic picture showing the setup of nanoindentation. A force is applied via an indenter to press the probe into the material of interest. The force applied is monitored through signal feedback from springs attached to the indenter. Figure adapted from "Nanoindentation", Cornell University (2014).

The material impression is converted into a single indentation value based on the force applied through the probe and the size of the material impression. The indentation value indicates the hardness, or rather the ability to resist plastic deformation, of the sample material [52]. Several parameters such as magnitude of applied force, tip shape and tip material can be tuned and the technique therefore offers a high levels of sensitivity [53].

2.9.2 Reverse Transcription – Polymerase Chain Reaction

The combination of reverse transcription (RT) and polymerase chain reaction (PCR) forms one of the most sensitive methods to detect gene expression currently available. The advantages are several since a RT-PCR can detect mRNA levels from very small samples [54] and also allows for evaluation of a large number of samples and detection of many different genes in the same experiment. The method is based on the denaturation of double stranded DNA chains by an increase in temperature whereupon the temperatures is lowered and primers are allowed to bind to target sequences on the single stranded DNA. This can also be done with samples containing single stranded RNA sequences in the corresponding procedure. Too high temperatures prevent the binding of primers, while too low temperatures promote non-specific binding of the primers. The temperature is again increased which initiate the production of complementary DNA (cDNA) chains through incorporation of dNTPs by RT enzymes. The reaction process in finished by once again increasing the temperature to obtain single-stranded cDNA [55]. The cDNA is exponentially amplified using PCR technique, resulting in the synthesis of large amounts of detectable double stranded DNA molecules representing the original sequence. There are many techniques available to quantify gene expression of the genes of interest but they all have in common that they link the amplification of cDNA to the generation of fluorescence, which can be easily detected during the PCR cycle. Hence, as the copies of the gene of interest increases during the reaction, so does the amount of fluorescence [55].

2.9.3 NBT/BCIP staining

Differentiation of pre-osteoblasts into mature osteoblasts is typically assessed by examining levels of ALP activity, which is identified as an early osteoblast marker. One way to evaluate the presence of ALP activity is by using colorimetric detection with a staining solution containing NBT (Nitro-blue tetrazolium chloride) and BCIP (5-bromo-4-chloro-3'-indolyphosphatase p-toluidine salt) [56]. ALP hydrolyses BCIP, which is further oxidized by atmospheric oxygen and NBT to form an insoluble dark blue precipitation.

2.9.4 Sirius Red F3B staining

Sirius Red F3B (2-Naphthalenesulfonicacid,7,7'-(carbonyldiimino)bis[4-hydroxy-3-[2-[2-sulfo-4-[2-(4-sulfophenyl)diazenyl]phenyl]diazenyl]-,sodium salt) is one of the best known staining techniques to detect presence of extracellular long fibres in a sample. It has further been reported suitable for quantitative measurements of collagen since the staining correlate well to the concentration of collagen [57]. The dye is strongly anionic due to the presence of sulfonic acid groups and has been reported to stain collagen type I and III well by reacting with the basic groups present in the collagen molecule [58].

2.9.5 Goldner's trichrome staining

Goldner's trichrome staining is frequently applied to visualize connective tissue and has been reported to generate excellent cellular resolution [59]. The staining solutions usually applied are Weigert's hematoxylin to stain the nuclei black, Ponceau Acid Fuchsin to stain unmineralized osteoid red and Light Green SF to stain the mineralized matrix green. The staining is based on the principle that smaller molecules penetrate the tissue structure faster than bigger molecules and by applying the staining dyes in a pre-determined sequence the different compartments of the bone tissue can be visualized simultaneously.

2.9.6 Alizarin Red S staining

The Alizarin Red S (3,4-Dihydroxy-9,10-dioxo-2-anthracenesulfonic acid sodium salt) is a frequently applied assay to quantitatively detect calcium deposits and visualize fine crystal structures in sample cultures [60]. The dye forms a complex with calcium in a chelating process and results in a detectable red precipitation. It should be noted that Alizarin Red S also reacts with elements such as magnesium, manganese, barium, strontium and iron but these are usually not present in sufficient amounts to interfere with the staining process of calcium.

2.10 Choice of substrate stiffness and culture time

The PA gel stiffnesses in this project were chosen based on the fact that the stiffness of mature cortical bone is in the range of GPa, while the stiffness of osteoid approximately is 20-40 kPa one week after secretion [49]. The latter value was used as a benchmark and substrates with stiffness around 4.8 kPa were chosen to represent newly laid down osteoid, substrates with medium stiffness around 19 kPa were chosen to simulate the reported stiffness of osteoid after one week and even stiffer substrates around 77 kPa would represent the bone matrix surface after additional time of osteoid mineralization. Some studies have attempted to further evaluate the impact of substrate mechanical properties on cell morphology, cytoskeletal assembly and differentiation. In a study conducted in 2006 by Discher *et al.* [49] an increase in substrate stiffness resulted in stiffer and more elongated morphology of the cultured cells. In that study, MSCs were cultured onto collagen coated polyacrylamide (PA) gels with stiffness 0.1, 1, 11 and 34 kPa. A change in morphology and phenotype of the cultured MSCs were observed before 7 days of culture. Cells cultured on the two softest and loose crosslinked gels showed a round morphology with dynamic focal adhesions and expressed neuronal markers while MSCs cultured on the two stiffer and more crosslinked gels showed an increased elongated morphology with stable focal adhesions and expressed myogenic markers (11 kPa) and osteogenic markers (34 kPa) without addition of enhancing differentiation medium. Also MC3T3-E1 cells have previously been applied in research aiming to evaluate substrate stiffness. In a study conducted by Putnam *et al.* in 2009 [68], these cells were cultured onto poly(ethylene glycol) (PEG) - based substrates with stiffness in the range of 14 kPa and 420 kPa. The impact of substrate stiffness was evaluated by determining the degree of differentiation and gene expression after 1, 7 and 14 days of culture. The stiffer substrate were shown to induce faster differentiation of the MC3T3-E1 cells and higher expression of bone formation factors collagen type I, ALP, bone sialoprotein and osteocalcin than the soft substrate already after 1 day of culture.

The impact of substrate stiffnesses in this project on MC3T3-E1 cell differentiation was evaluated after 24 hours, 72 hours and 7 days, since time points within one week previously had been proven sufficient by Putnam *et al.* [68] to detect a difference in differentiation for these cells. In the same study, gene expression was detected after 1 day of MC3T3-E1 cell culture, but since the stiffer substrate (420 kPa) in that study greatly exceeded the stiffest substrate applied during this project 48 hours of culture prior to gene expression detection were instead applied. This culture time was also chosen before evaluation of proliferation due to practical reasons with RNA isolation. Detection of metabolic activity (after 7 days of culture) and matrix mineralization (13 days) were based on previous studies where substrate stiffness was observed to affect the metabolic activity of primary osteoblast after 7 days [61] and matrix mineralization was observed for osteogenic cells within two weeks of culture [44].

3. Materials and methods

3.1 MC3T3-E1 culture maintenance

The cell line used for all experiments was pre-osteoblast MC3T3-E1 cells. It was maintained throughout the project at sub-confluent concentrations in T175 cm² culture flasks (Sigma-Aldrich, the United States), using an incubator system (DJB Labcare, the United Kingdom) at 37°C and 5% CO₂. The MCT3T-E1 cells were grown in α -MEM culture medium supplemented with 10% fetal bovine serum (FBS), 1% vitamin C, 1% L-glutamine, 0.5% fungizone, 0.25% penicillin and 0.25% streptomycin. Media changes and/or cell passaging were performed every 3-4 days. Complete protocols for cell passaging and seeding can be found in Appendix A.1, A.5 and A.6.

3.2 Preparation of MC3T3-E1 substrates

In order to evaluate the influence of ECM stiffness on seeded MC3T3-E1 cells, polyacrylamide (PA) gels with different stiffness and partly demineralized bone pieces were applied as cell substrate. Stiffer PA gels were produced by increasing the initial concentration of the two monomers acrylamide and bis-acrylamide and detailed protocols for the substrate preparation procedures can be found in Appendix A.3 and A.4.

3.2.1 Cow bone demineralization with EDTA

Cow bone pieces of approximately 9 mm² were kindly provided by Academic Centre Dentistry Amsterdam (ACTA) and detailed protocol concerning the demineralization process can be found in Appendix A.2. Briefly, the bone pieces were kept in a 96-well plate and demineralized in aqueous solution of EDTA (4.2% EDTA in distilled water, pH 7.0). The EDTA was changed every third day and two bone pieces were at the same time removed from the EDTA solution and replaced in PBS, with an addition of 250 μ l Antibiotic Antimycotic Solution (Sigma-Aldrich, the United States). Replicates of bone pieces were subject to EDTA treatment in two sets of different time points. The first set yielded bone pieces with 0, 6, 12, 24, 48, and 72 hours of demineralization and the second set resulted in replicates of bone pieces with 0, 4, 7, 11, 14, 18 and 21 days of demineralization. Bone pieces lacking demineralization were kept in PBS throughout the demineralization period in the two sets.

3.2.2 Fabrication and functionalization of PA gels

Model substrates were fabricated from polyacrylamide (PA) according to protocol found in Appendix A.3. Briefly, the cover glasses (15 mm in diameter) were prepared by placing them in a beaker containing acetone and silane (3-(Trimethoxysilyl)propyl methacrylate). The silane functions as a coupling agent to facilitate subsequent attachments of the PA gels onto the surface of the cover glass. The beaker was gently tilted during 20 minutes (Microplate Shaker®, VWR, the United States). The cover glasses were then replaced into a

beaker containing pure acetone and put on the shaker for another 10 minutes. The cover glasses were allowed to dry and subsequently placed in PBS at 4°C until used.

Stock solutions of 40% acrylamide (Bio-Rad, the United Kingdom) and 2% *N,N'*-methylene-bis-acrylamide (Bio-Rad, the United Kingdom) were combined to yield sets of PA gels with an estimated final stiffness in the range of 4.8 kPa for the softest PA gel, 19 kPa for the medium and 77 kPa for the stiffest PA gel. The PA solutions were prepared in distilled water with an addition of the free radical stabilizer TEMED [1,2-di-(dimethylamino) ethane] (Bio-Rad, the United Kingdom). Following the addition of 10% ammonium persulfate the solution were immediately placed as drops onto a hydrophobic glass plate, covered with glass cover slips and allowed to polymerize. Following polymerization, the gels with the glass cover slip were flipped and placed in the wells of a 24-well plate, as presented in Figure 8.

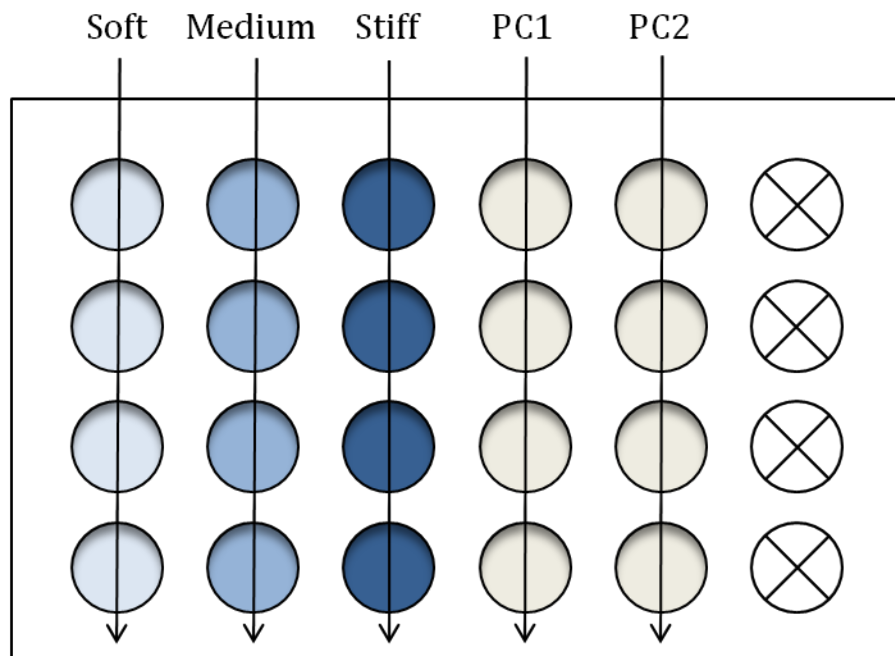


Figure 8. Schematic picture showing the resulting arrangement of PA gel substrates with different stiffness and the plastic control (PC1 and PC2) in the wells of 24-well plate. All of the substrates are subsequently coated with collagen type I.

Gels were functionalized to support cell adhesion by covalently attach a coating of collagen type I according to protocol found in Appendix A.4. Briefly, the UV-light sensitive cross-linker sulfo-SANPAH [*N*-sulfosuccinimidyl-6-(4'-azido-2'-nitrophenylamino) hexanoate] was via its azide functionality covalently attached to the otherwise inert PA gel surface. A solution of 1.0 mM sulfo-SANPAH prepared in 50 mM Hepes (pH 7.4) was added to the PA gel surface and a reaction was immediately induced by exposing the gels to UV-light (UV Transilluminator, UVP, the United Kingdom) for 8 minutes. Following UV-light treatment, the PA gels were washed with 50 mM Hepes (pH 7.4) and the photo activation treatment was repeated. Next, the gels were again washed two times with 50 mM Hepes (pH 7.4), to remove excess sulfo-SANPAH reagent. A solution of collagen type I (0.1 mg/ml) in PBS was added to the polyacrylamide gels, which were allowed to incubate overnight at 4°C. The following day the gels were washed with PBS twice and stored in PBS with an addition of Antibiotic antimycotic solution (Sigma-Aldrich, the United States) at 4°C until used.

3.2.3 Fabrication and functionalization of plastic control substrates

Plastic control substrates were functionalized to support cell attachment according to protocol found in Appendix A.4. Briefly, the plastic surfaces were washed with milliQ water and placed in a solution of PBS and 0.5% glutaraldehyde, which was done to enhance the subsequent attachment of the collagen coating to the plastic surface. After additional washing steps the plastics were allowed to dry in the laminar flow cabinet. The plastic control substrates were coated with collagen type I (0.1 mg/ml) to support cell adhesion in the same procedure as previously described for the PA gel substrates. The plastic controls were stored in PBS with an addition of Antibiotic antimycotic solution (Sigma-Aldrich, the United States) at 4°C until used. The resulting plate with both coated PA gels and plastic controls is presented in Figure 8.

3.2.4 Determined stiffnesses of the PA gels

The precise stiffness of the three different PA gels was measured with nanoindentation (Piuma, the Netherlands) according to manufacturer's instructions. The probe used had a stiffness of 0.62 N/m, an amplitude of 2 V and a tip radius of 35 µm. All measurements were conducted in water to minimize the adhesion effect between the applied probe and the PA gel surface. The measurements were conducted four times at three different spatial positions on the PA gels to maximize the accuracy of the obtained overall stiffness values.

3.3 MC3T3-E1 cell experiments

Prior to MC3T3-E1 cell seeding, all substrates were incubated (DJB Labcare, the United Kingdom) with MCT3T-E1 culture medium at 37°C and 5% CO₂ for one hour. Passages under 36 were used in all experiments. In the experiments with PA gels 1 nM vitamin D [1.25(OH)₂ vitamin D₃] was added to the second column of plastic controls (PC2 in Figure 8), which as a result is designed the abbreviation PCD in the Results section. The fourth row in Figure 8 was seeded with MC3T3-E1 cells but used as negative control in all performed experiments with PA gels as substrates. A cell seeding concentration of 5000 cells/cm² was applied in all MC3T3-E1 cell experiments except when aiming to evaluate the degree of matrix mineralization induced by the MC3T3-E1 cells (see section 2.9.6). In that case a higher cell seeding concentration of 10 000 cells/cm² was used to shorten the proliferation time and accelerate differentiation among the seeded MC3T3-E1 cells. The culture medium was refreshed every second day. Detailed protocol of experimental procedures can be found in Appendix A.5 and A.6.

3.4 Gene expression of valid bone formation markers

In order to determine the effect from the different substrates on metabolic and gene expression level of MC3T3-E1 cells the total amounts of RNA, DNA and protein were determined and a RT-PCR conducted. The MC3T3-E1 cells were seeded with an initial cell seeding concentration of 5000 cells/cm² onto both PA gels, as presented in Figure 8, and partly demineralized bone and the samples were evaluated after 48 hours of culture. For the demineralized bone, the pieces were prior to detection replaced in new wells. Attempts to measure levels of total protein were conducted for both PA gel substrates and demineralized bone pieces with a Micro BCA™ Protein Assay Kit (Thermo Scientific, the United States) according to manufacturer's instructions. The levels were however too low to enable detection. Detailed protocols for the experimental procedures can be found in Appendix A.7 and A.8.

3.4.1 Isolation of RNA

The samples were treated according to protocol found in Appendix A.7. In brief, the samples were washed with PBS three times and treated with Trizol. Chloroform was added to the resulting solution and the samples were centrifuged (Hettich Zentrifugen, Germany). As a result of the centrifugation treatment, two phases were obtained. The upper water phases contained the RNA and the lower organic phases contained the DNA and proteins. The two phases were separated by gently removal of the water phases into a new set of tubes. The organic phases were placed in -80°C until use for DNA isolation while the water phases were once again centrifuged. The resulting supernatants were discarded and the pellets washed with an addition of 75% ethanol, followed by centrifugation. The pellets were carefully dried by removal of surrounding liquid and subsequently diluted with

distilled water. To obtain complete dilution of the RNA pellet the samples were put in a water bath (Salm en Kipp, the Netherlands) at 57°C before the RNA content was quantified with conventional 260/280 absorbance readings (Bio-Tek, the United States), using the analysis software Gen5™ (Bio-Tek, the United States) according to manufacturer's instructions.

3.4.2 Isolation of DNA

The samples with the organic phases stored from the isolation of RNA in section 3.4.1 was further isolated according to protocol found in Appendix A.7. Briefly, 100 % ethanol was added to each sample and they were allowed to incubate at room temperature before centrifugation (Hettich Zentrifugen, Germany). The resulting supernatants were transferred into a new set of tubes and stored in -80°C until used for protein isolation. Sodium citrate was added to the remaining pellets and the samples were allowed to incubate at room temperature, followed by centrifugation. The sodium citrate was thereafter discarded and the incubation and centrifugation procedure repeated. The resulting pellet was dissolved in 75% ethanol. The samples were thereafter incubated at room temperature before centrifugation. The supernatants were discarded and the remaining pellets left to dry at room temperature. When completely dry, the pellets were dissolved in sodium hydroxide and the samples were once again centrifuged. The resulting supernatants were transferred into a new set of tubes and placed in a water bath (Salm en Kipp, the Netherlands) at 57°C. The DNA content was quantified with conventional 260/280 absorbance readings (Bio-Tek, the United States), using the analysis software Gen5™ (Bio-Tek, the United States) according to manufacturer's instructions.

3.4.3 Isolation of proteins

The supernatant from the DNA isolation in section 3.4.2 was further treated according to protocol in Appendix A.7. In brief, isopropanol was added to the samples and they were incubated at room temperature before centrifugation (Hettich Zentrifugen, Germany). The supernatants were discarded and the pellets incubated at room temperature with guanidine hydrochloride in 95% alcohol. After incubation the samples were centrifuged and the supernatants were carefully removed. This was repeated three times followed by addition of 100% ethanol and vortex treatment. The samples were allowed to incubate at room temperature before centrifugation. The supernatants were discarded and the remaining pellets were left to dry at room temperature. When completely dried pellets had been obtained, they were dissolved in 1% sodium dodecyl sulphate (SDS) and incubation at 50°C to obtain completely dissolved pellets. The resulting samples were centrifuged and the supernatants transferred into a new set of tubes. The samples were stored at -20°C until the protein content was determined using Micro BCA™ Protein Assay Kit (Thermo Scientific, the United States) and absorbance readings at 562 nm (Bio-Tek, the United States) with analysis software Gen5™ (Bio-Tek, the United States), according to manufacturer's instructions.

3.4.4 Detection of gene expression of bone formation markers

The MC3T3-E1 cell gene expressions of bone sialoprotein, collagen type I, ALP, osteocalcin and osteopontin were evaluated according to protocol found in Appendix A.8. In brief, the isolated RNA (see section 3.4.1) was converted into cDNA using a cDNA synthesis kit (Thermo Scientific, the United States) and Gene Amp[®] PCR System 9700 (Life Technologies, the United States). A RT-PCR was performed with primers (Thermo Scientific, the United States) for bone sialoprotein, collagen type I, ALP, osteocalcin, osteopontin and the two housekeeping genes ymHAZ and HPRT with a LightCycler[®] analyser (Roche, Switzerland).

3.5 Detection of ALP activity

To evaluate time dependent differentiation induced by the stiffness of the culturing substrates the MC3T3-E1 cells were seeded with a concentration of 5000 cells/cm² onto three separate PA gel plates (see Figure 8). These plates were stained for ALP activity after 24 hours, 72 hours and 7 days respectively. Detailed protocol for the staining procedure can be found in Appendix A.9. In brief, the cells were fixated with 4% formaldehyde in PBS and a stock solution containing NBT/BCIP (Roche, Switzerland) was added. The plate was allowed to incubate at 37°C and the staining solution was then removed and the samples washed repeatedly with distilled water. To optimize the removal of unspecific staining the wells were further left overnight with distilled water. The results were examined with 10x magnification using optical microscopy (Leica, Germany).

3.6 Staining with Sirius Red F3B

The presence of extracellular collagen type I was evaluated by seeding MC3T3-E1 cells onto one PA gel plate (see Figure 8) with an initial cell seeding concentration of 5000 cells/cm². The plate was stained with Sirius Red F3B after 7 days of culture and detailed protocol can be found in Appendix A.10. Briefly, the cells were fixated with 4% formaldehyde in PBS and a solution of 0.1% Sirius Red F3B (BDH Chemicals, the United Kingdom) in saturated aqueous solution was added to each well and allowed to stain in room temperature. Following staining, the wells were repeatedly washed with acidified water. To optimize the removal of un-bound Sirius Red F3B dye the wells were also rinsed with 100% ethanol. The results were examined with 10x magnification using optical microscopy (Leica, Germany).

3.7 Staining with Alizarin Red S

To accelerate differentiation and mineralization of the MC3T3-E1 cells a higher initial concentration of 10 000 cells/cm² were seeded onto one PA gel plate (see Figure 8) and induced mineralization of the ECM was analysed after 13 days of culture. This was done using an Alizarin Red S assay, as described in protocol found in Appendix A.11. In brief, the cells were rinsed with PBS twice before being fixated with 4% formaldehyde in PBS. The

plate was incubated with 2% Alizarin Red S solution (Sigma Aldrich, Germany) in room temperature. Following incubation, the solution was removed and the plate placed on a microplate shaker, followed by washing with pipe water, to remove any unbound Alizarin Red S. To optimize the removal of unspecific staining the wells were left overnight with tap water. The results were examined with 4x magnification using optical microscopy (Leica, Germany).

3.8 Staining with Goldner's trichrome

The distribution of osteoid, mineralized matrix and cell nuclei of the partly demineralized bone pieces was evaluated with Goldner's trichrome staining according to protocol found in Appendix A.12. In brief, the MC3T3-E1 cells were seeded onto the partly demineralized bone pieces with an initial concentration of 5000 cells/cm². After 48 hours of culture, the samples were fixated with 4% formaldehyde in PBS. The staining solution Weigert's Hematoxylin (Life Technologies, the United States) was added and the samples were allowed to incubate in room temperature. Following incubation, the samples were rinsed with distilled water and incubated with tap water at room temperature prior to addition of the second staining solution. Ponceau Acid Fuchsin (Life Technologies, the United States) was added and the samples were allowed incubation before repeated wash with acetic acid. The last staining, Light green SF solution (Life Technologies, the United States), was added to each sample and they were once again allowed to incubate at room temperature prior to finishing washing steps with distilled water and ethanol (75% and 100%).

The resulting staining yield:

Table 2. Colour distribution in Goldner's trichrome staining.

Stained structure	Resulting colour
Cell nuclei/Unspecific matrix	Dark blue to black
Mineralized matrix	Green
Osteoid	Red

3.9 Statistical analysis

Measurements of total RNA and DNA levels were performed in triplicates on three identical sample substrates for the MC3T3-E1 cells seeded onto PA gels and plastic controls. For the MC3T3-E1 cells with the partly demineralized bone pieces as substrates, measurements were conducted in replicates on two identical bone piece samples. Measurements of gene expression of chosen bone formation markers were conducted in replicates on three identical substrates. Evaluation of PA gel stiffnesses were conducted four times at three different spatial gel positions. The mean value of all obtained data is presented with \pm SD and statistical significance was assessed using Student's t-test.

4. Results

4.1 Stiffness of the PA gels used

The stiffness of the PA gel substrates were measured with nanoindentation to evaluate if they were in the range expected from the production process. The expected stiffness values were based on previous research conducted at ACTA, Amsterdam with the same mixing ratio of acrylamide and bis-acrylamide as used in this project. The actual stiffness of the PA gels had however never before been confirmed with nanoindentation and the average results from these measurements are presented in Figure 9 and Table 3.

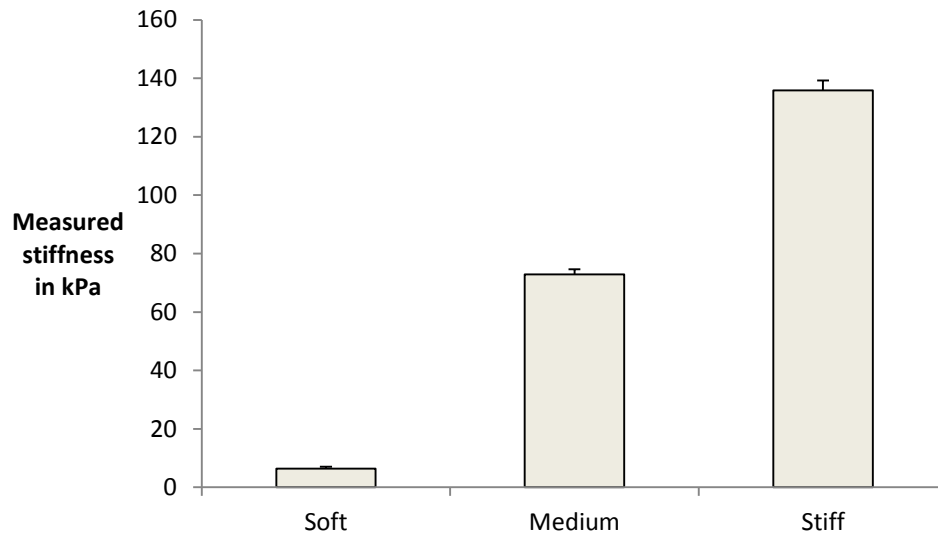


Figure 9 . The measured stiffnesses of the soft, medium and stiff Pa gels with nanoindentation.

The expected stiffness of the softest PA gel was 4.8 kPa but measurements revealed that the actual stiffness was 6.4 ± 0.7 kPa, which is 33% higher than expected. Similar results were observed for the medium and stiffest PA gel, which were expected to have stiffnesses in the range of 19 and 77 kPa. However, the actual stiffnesses for these PA gels were 72.9 ± 1.7 and 135.9 ± 3.4 , which corresponds to 384% and 176% of the expected stiffnesses, respectively.

Table 3. The expected and actual measured stiffness of the produced PA gels presented in mean kPa \pm SD.

Expected stiffness (kPa)	Measured stiffness (kPa)
4.8	6.4 ± 0.7
19	72.9 ± 1.7
77	135.9 ± 3.4

4.2 Substrate stiffness dictate osteoblast morphology

The impact of substrate stiffness on MC3T3-E1 cell morphology was investigated after 24 hours of culture and the results are presented in Figure 10. On the softest PA gel the MC3T3-E1 cells have a more rounded morphology than on the stiffer substrates. As expected, the more elongated morphology for the cells cultured on the medium and stiff PA gels and the plastic controls shows higher degree of cell attachment on these stiffer substrates. Further a more extensive proliferation was observed for cells seeded onto the stiff PA gel and the two plastic controls (PC and PCD). No difference in cell morphology or proliferation could be observed between PC and PCD, which indicates a subordinate influence of vitamin after 24 hours.

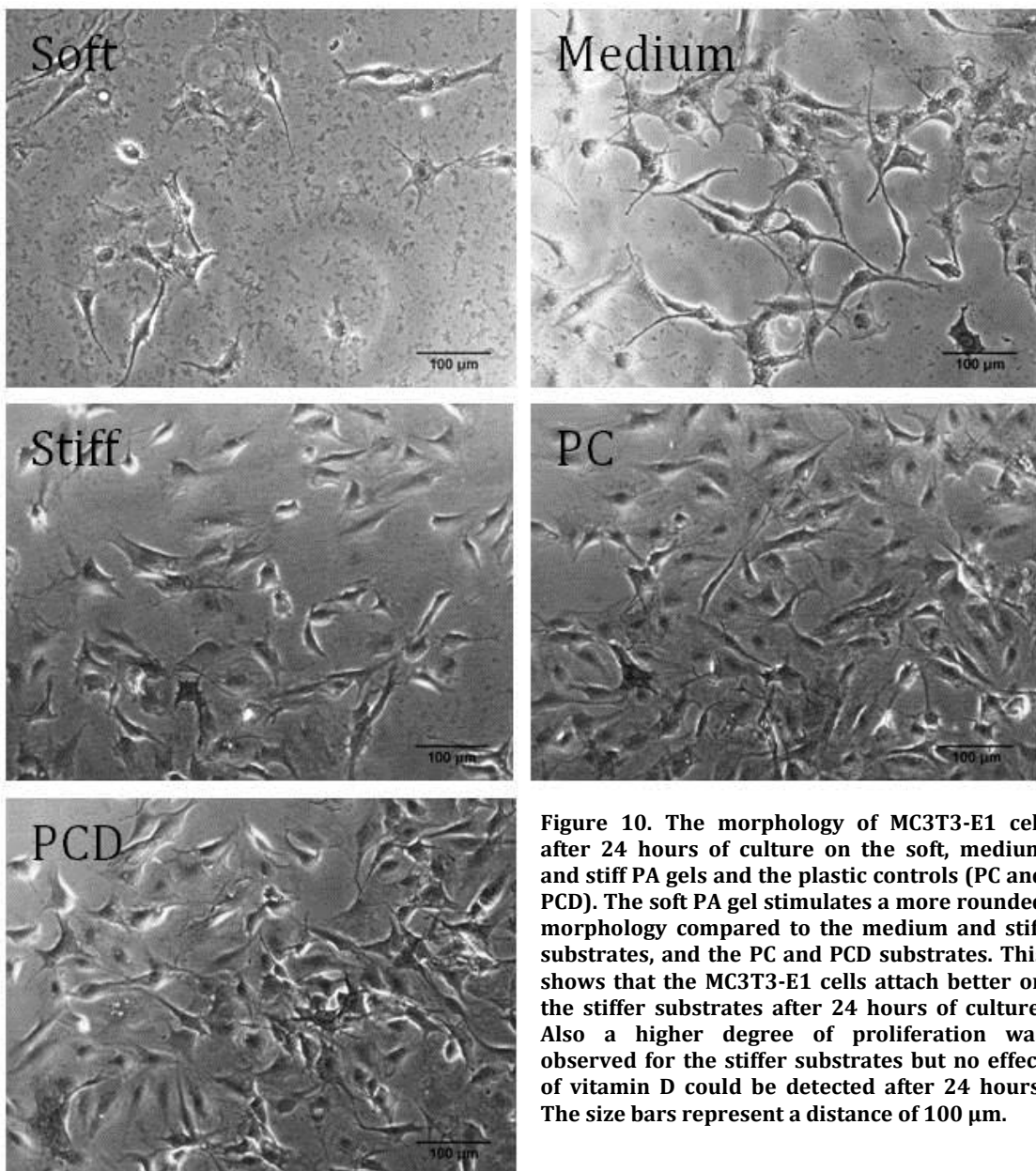


Figure 10. The morphology of MC3T3-E1 cell after 24 hours of culture on the soft, medium and stiff PA gels and the plastic controls (PC and PCD). The soft PA gel stimulates a more rounded morphology compared to the medium and stiff substrates, and the PC and PCD substrates. This shows that the MC3T3-E1 cells attach better on the stiffer substrates after 24 hours of culture. Also a higher degree of proliferation was observed for the stiffer substrates but no effect of vitamin D could be detected after 24 hours. The size bars represent a distance of 100 µm.

4.3 Osteoblast proliferation on substrates with various stiffness

To evaluate the impact of substrate stiffness on MC3T3-E1 cell proliferation, both levels of total RNA and DNA were detected for cells seeded onto the soft, medium and stiff PA gel substrates. The stiffness was not observed to influence the levels of total RNA detected for the three sample stiffnesses after 48 hours of culture, as seen in Figure 11. The soft, medium and stiff substrates all presented levels of total RNA in the span 100 to 120 ng/ μ l. The detected RNA levels indicated an up-regulated proliferation for the MC3T3-E1 cells seeded onto plastic control without added vitamin D (PC), with a twofold increase compared to the levels detected for the three substrates and plastic control with added vitamin D (PCD). These results indicate that vitamin D does not function as an enhancer of MC3T3-E1 cell proliferation after 48 hours of culture. No statistically significant difference between the different substrates and plastic controls could however be established.

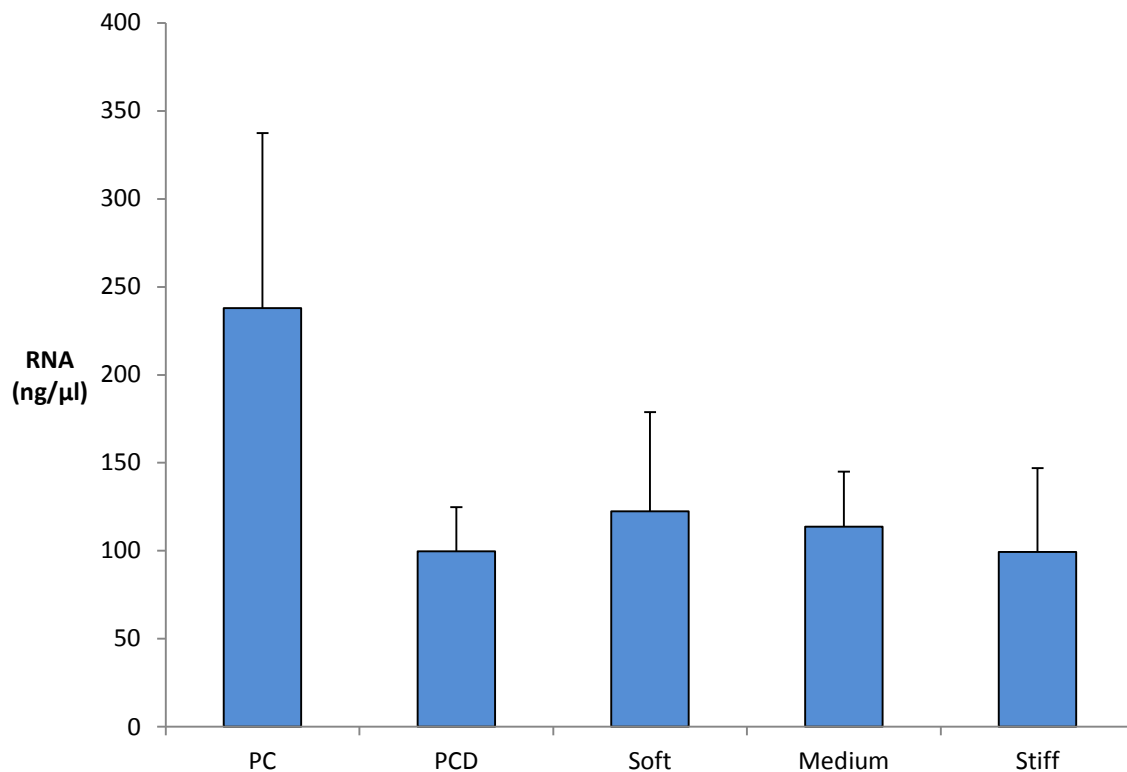


Figure 11. The detected levels of total RNA presented in ng/ μ l for MC3T3-E1 cells seeded with concentration 5000 cells/ cm^2 onto the PA gels with three different stiffnesses and plastic controls.

The levels of total DNA were further detected for the three substrate stiffnesses and plastic controls after 48 hours of culture. Similar levels of total DNA were observed for the MC3T3-E1 cells seeded onto all substrates and plastic controls (PC and PCD). The mean levels for all substrates were detected in the span between 30 and 40 ng/ μ l, as presented in Figure 12. In contrast to the total levels of RNA, no up-regulation in proliferation was observed for the MC3T3-E1 cells seeded onto the PC substrates. No enhancing effect of vitamin D in proliferating of MC3T3-E1 cells after 48 hours of culture was detected for the levels of total DNA.

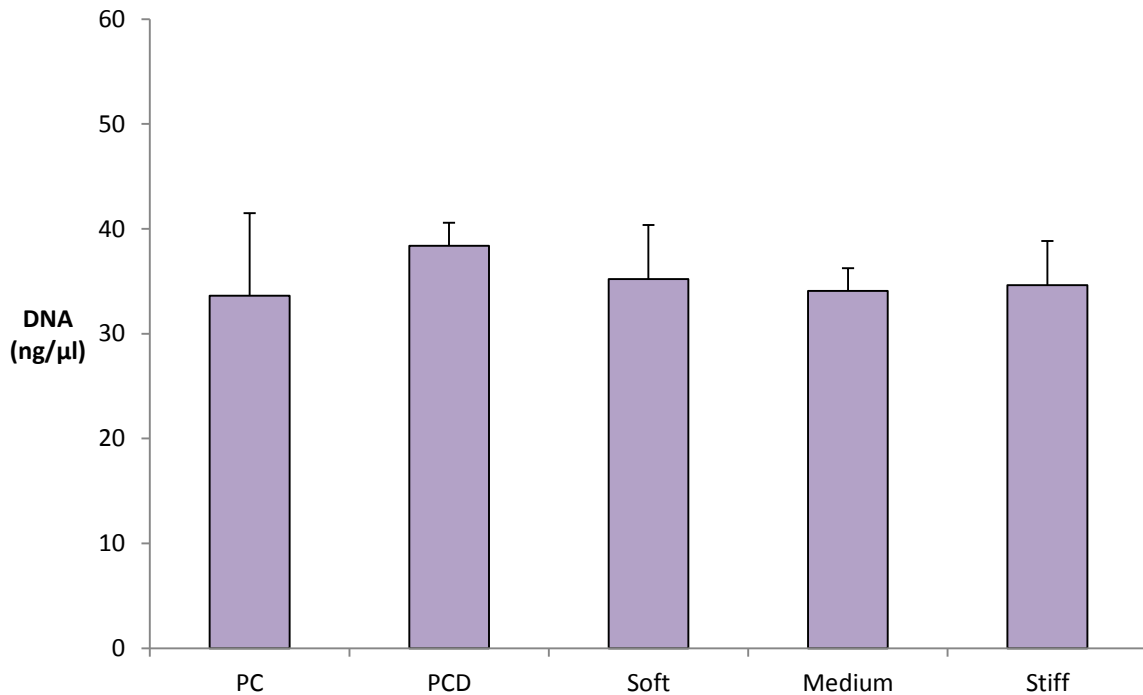


Figure 12. The detected levels of total DNA presented in ng/ μ l for MC3T3-E1 cells seeded with concentration 5000 cells/ cm^2 onto the PA gels with three different stiffnesses and plastic controls.

4.4 Osteoblast differentiation on substrates with various stiffness

Alkaline phosphatase (ALP) activity is a marker for early osteoblast differentiation. To determine how substrate stiffness affect time dependent MC3T3-E1 cell differentiation the levels were evaluated qualitative after 24 hours, 72 hours and 7 days of culture. The results are presented in Figure 13. At none of the chosen time points ALP activity could be detected on the soft and medium substrates, while the levels of ALP activity on the stiffest substrates was observed already after 24 hours of culture. As expected, this was also the case with the plastic controls, where the ALP activity increased continuously for the duration of the culture. Plastic substrate with an addition of vitamin D (PCD) was found to induce the highest degree of ALP activity. This confirms that vitamin D function as an enhancer of MC3T3-E1 cell differentiation and that the effect becomes more evident with time. As a result the highest levels of ALP activity were detected for the MC3T3-E1 cells cultured onto PCD substrates after 7 days of culture. Images were taken with 10x magnification using a Leica DFC 320 (Leica, Germany).

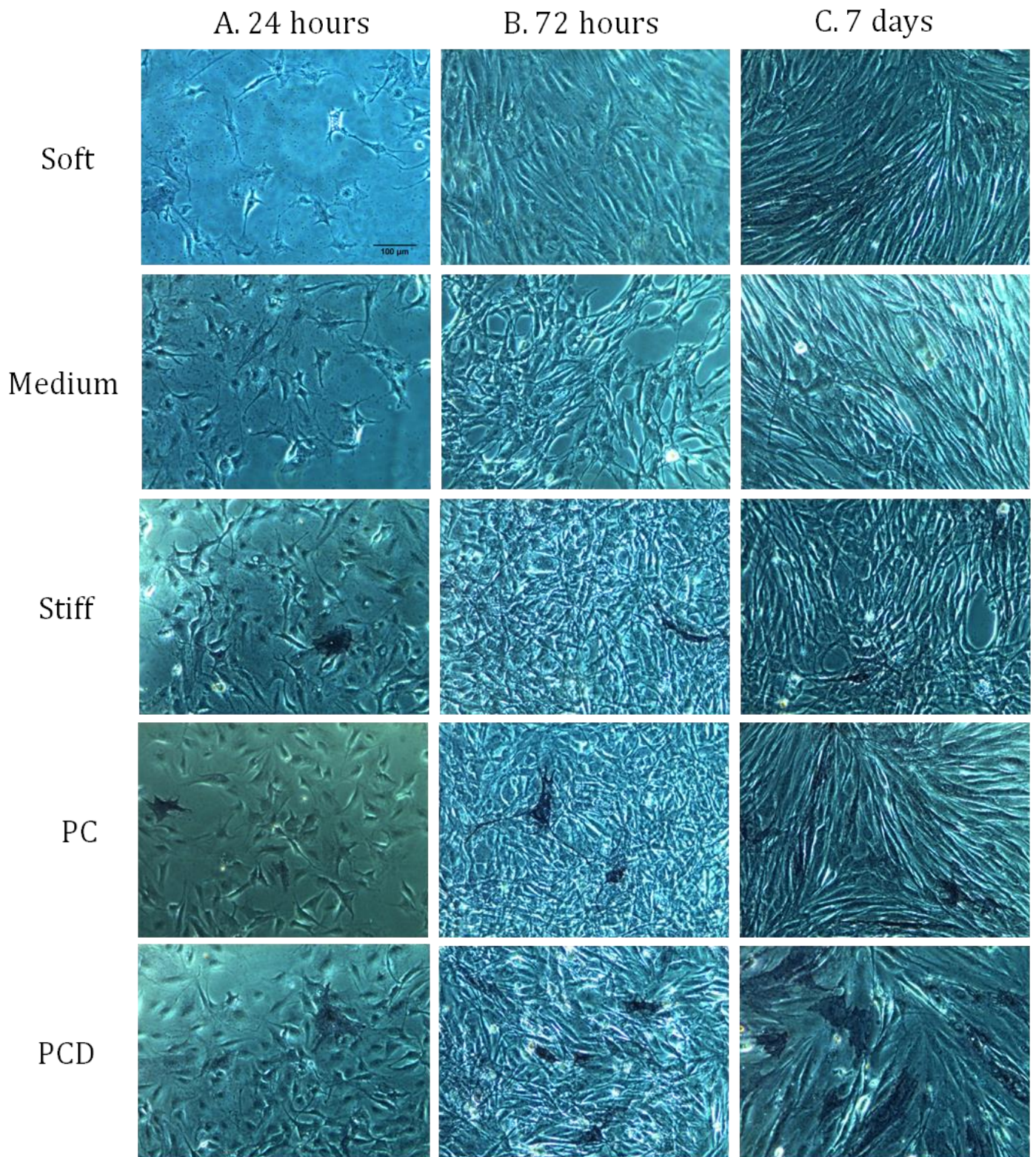


Figure 13. MC3T3-E1 cells stained for ALP activity after 24 hours, 72 hours and 7 days of culture. ALP activity can be observed as darker areas of blue staining. No ALP activity could be detected for the MC3T3-E1 cells cultured on the softest or medium PA gels. Increasing ALP activity was observed on the stiffest PA gel and the plastic controls (PC and PCD) with time. The size bar in photo (A) for the soft gel represent 100 µm and is applicable for all images above.

4.5 Gene expression of bone formation markers

A RT-PCR was performed to detect the presence of five well known osteoblast products after 48 hours, with the result presented in Figure 14. Similar levels of gene expression of collagen type I, bone sialoprotein and osteopontin were observed for the soft, medium and stiff substrates, indicating a subordinate importance of the substrate stiffness in the MC3T3-E1 cell gene expression of these osteoblast markers. The expressions of all detected markers were up-regulated for the plastic controls (PC and PCD) compared to the samples substrates. A slight down-regulation in gene expression between PC and PCD indicates that vitamin D does not function as a positive control for the gene expression of collagen type I, bone sialoprotein and osteopontin in MC3T3-E1 cells after 48 hours. No gene expression of alkaline phosphatase or osteocalcin could be detected for any of the substrates.

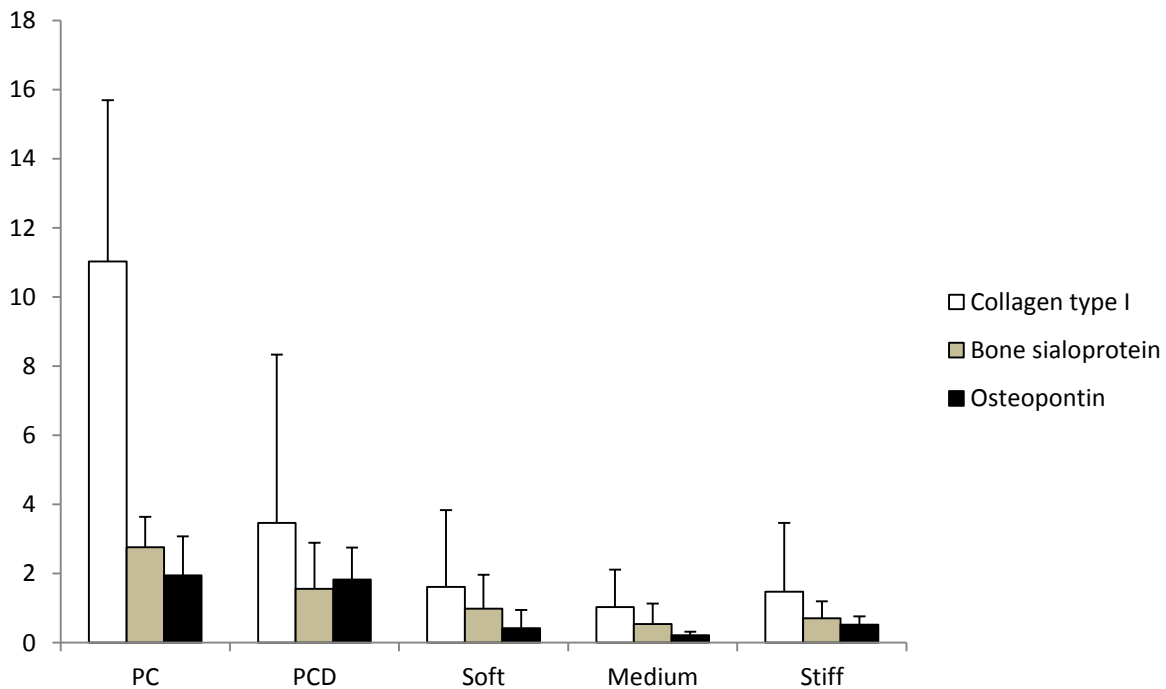


Figure 14. Detected levels of collagen type I, bone sialoprotein and osteopontin for the three substrate stiffnesses and plastic controls (PC and PCD) after 48 hours of MC3T3-E1 cell culture. No expression of alkaline phosphatase and osteocalcin was observed for any of the samples. No difference in levels of gene expression can be detected between the three sample stiffnesses.

4.6 Impact of substrate stiffness on osteoblast metabolic activity

Staining with Sirius Red F3B was performed to detect the presence of extracellular collagen type I after 7 days of MC3T3-E1 cells culture. Photos were taken with 10x magnification using a Leica DFC 320 (Leica, Germany) microscope and the results for the three substrate stiffnesses and plastic controls are displayed in Figure 15A-E. The PA gels without seeded MC3T3-E1 cells (see row 4 in Figure 8) were also stained with Sirius Red F3B as control and is shown for the stiffest sample substrate in Figure 15F. The collagen type I coating was distinguished as darker areas of grey. This dark grey staining was not observed for any of the substrates seeded with osteoblasts, which shows that the collagen type I coating is degraded by the MC3T3-E1 cells within 7 days of culture. The grey staining of the coating was distinguished from a red staining of intracellular matrix and nucleus of the MC3T3-E1 cells. No extracellular collagen type I indicated secretion of osteoid at any of the substrate stiffnesses or plastic controls after 7 days of culture.

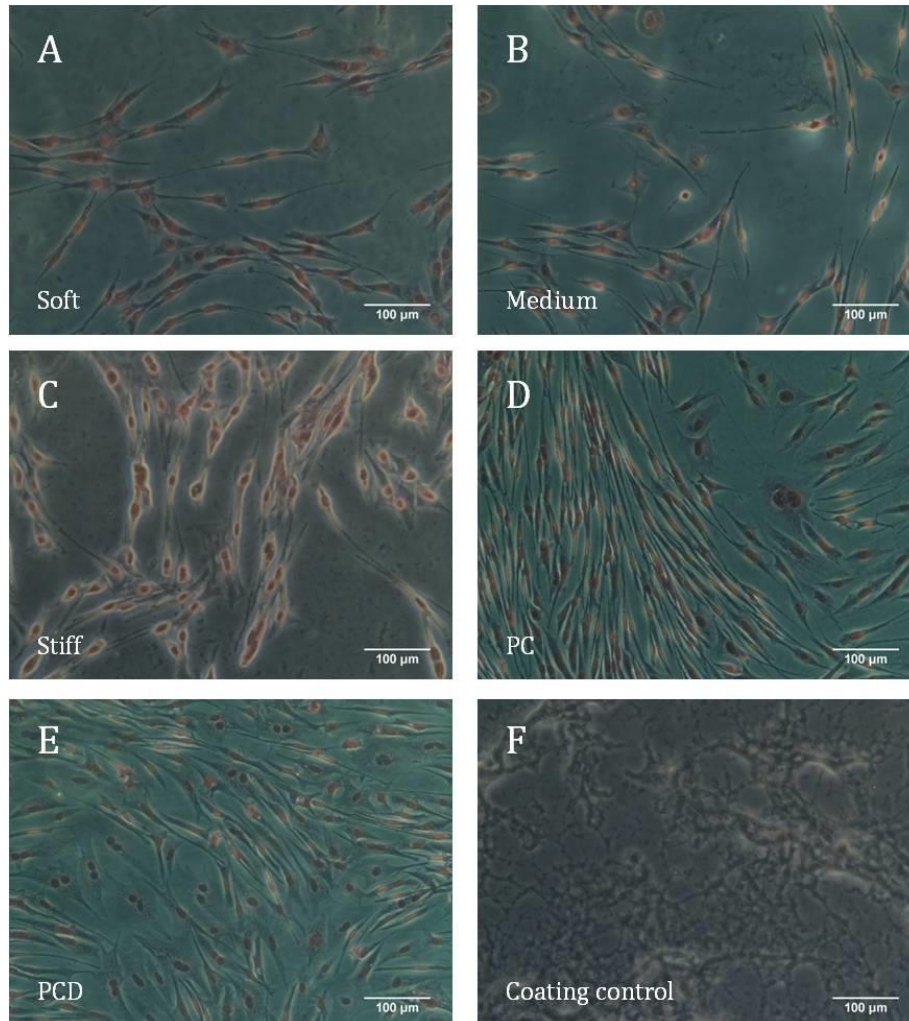


Figure 15. Staining with Sirius Red F3B shows the remaining collagen type I coating after 7 days of MC3T3-E1 cell cultures. The cells are visualized in red while collagen type I coating are seen as darker areas of grey. (A) - (E) The three substrate stiffnesses and plastic controls. (F) The control without seeded MC3T3-E1 cells on the stiffest sample substrate. The size bars represent a distance of 100 µm.

4.7 Matrix mineralization induced by substrate stiffness

Induced matrix mineralization by MC3T3-E1 cells was investigated with Alizarin Red S staining and the results are presented in Figure 16. No mineral production was observed on the soft, medium or stiff substrates after 13 days of culture. Calcium nodules were only observed in the plastic control samples which had received an addition of vitamin D (PCD), which is presented in Figure 16A. A representative picture of the absence of matrix mineralization is presented for the PA gel substrate with medium stiffness in Figure 16B. Images were taken with 4x magnification using a Leica DFC 320 (Leica, Germany).

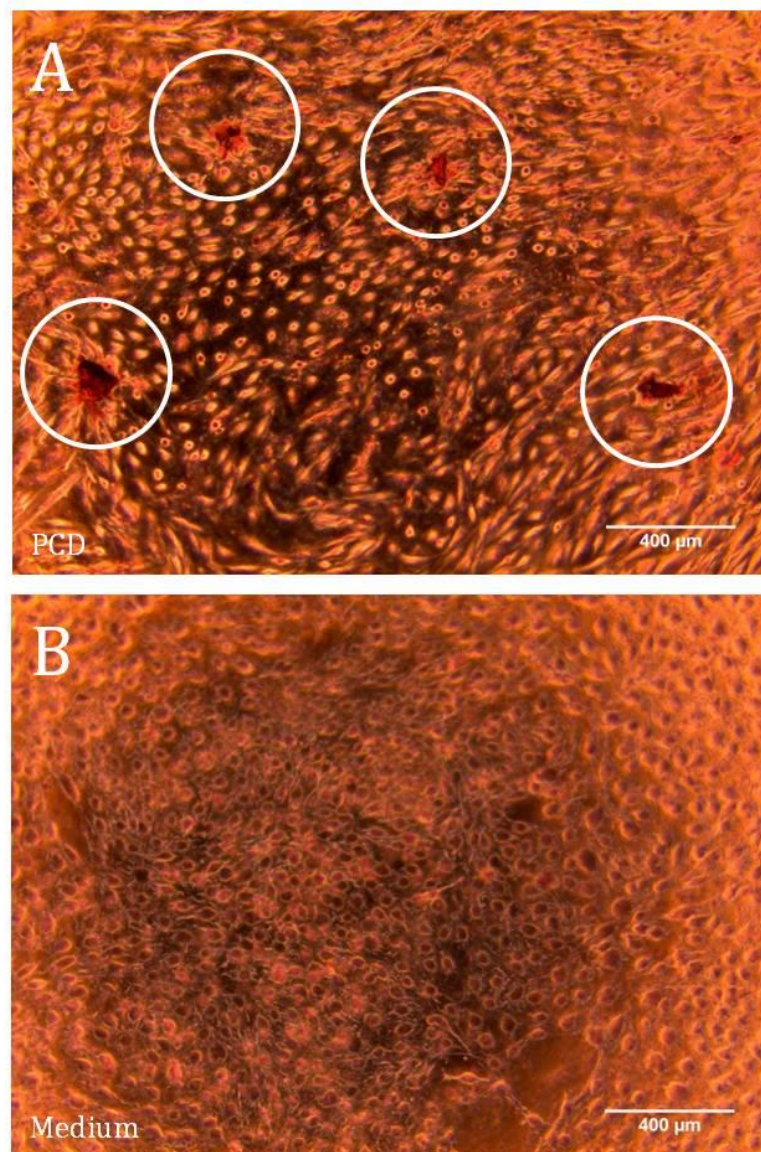


Figure 16. The resulting staining of MC3T3-E1 cells with Alizarin Red S after 13 days of culture. Formation of calcium nodules was only detected for the MC3T3-E1 cells cultured on PCD substrate, which is highlighted with white circles in (A). The lack of matrix mineralization is presented in a representative picture for the PA gel with medium stiffness (B).

4.8 Demineralization of bone pieces

Bone pieces from cow were demineralized for 6, 12, 24, 48 and 72 hours and further for 4, 7, 11, 14, 18 and 21 days. After finished demineralization treatments the samples were seeded with MC3T3-E1 cells and stained with Goldner's trichrome after 48 hours of culture. The results are presented for chosen time points in Figure 17. Photos were taken with 10x magnification using a Leica DFC 320 (Leica, Germany) for Figure 17A-D, while Figure 17E-F were taken with conventional camera through the lens of a Zeiss Light Microscope (Zeiss, Germany).

A control bone piece lacking demineralization is presented in Figure 17A, where the fine structures and Haversian canals can be observed as darker areas together with incorporated osteocytes in the green mineralized matrix. The bone sample in Figure 17B has been demineralized for 6 hours and the presence of unidentified structures was observed as red unmineralized flakes (examples of these flake structures are indicated with white arrows in Figure 17) above the green mineralized bone surface. An expected demineralization pattern was first observed after 48 hours of demineralization treatment, as seen in Figure 17C. This type of demineralization was observed at the edges of the bone pieces with yellow staining indicating progressing demineralization and red staining show areas of completely demineralized bone matrix. Together with the expected bone demineralization the flake structures were observed throughout the first demineralization process (until 72 hours of demineralization), as presented after 48 hours in Figure 17D. In Figure 17E the resulting staining after 4 days of demineralization is presented. Severe demineralization was observed, where the unmineralized matrix and cell nuclei are amply stained. This results in difficulties to distinguish different components of the bone tissue and precluded photos with high magnification. It cannot be excluded that the observed flakes are a contributing factor to the extensive staining observed. After 21 days of demineralization treatment the effect is even more evident, as seen in Figure 17F.

An increased degree of MC3T3-E1 cell migration from the softer bone tissue to the underlying plastic was observed with increasing demineralization time, which is shown for the samples after 4 and 21 days of demineralization in Figure 17E-F. Observe that the size bars used in Figure 17A-D differs from the ones in Figure 17E-F.

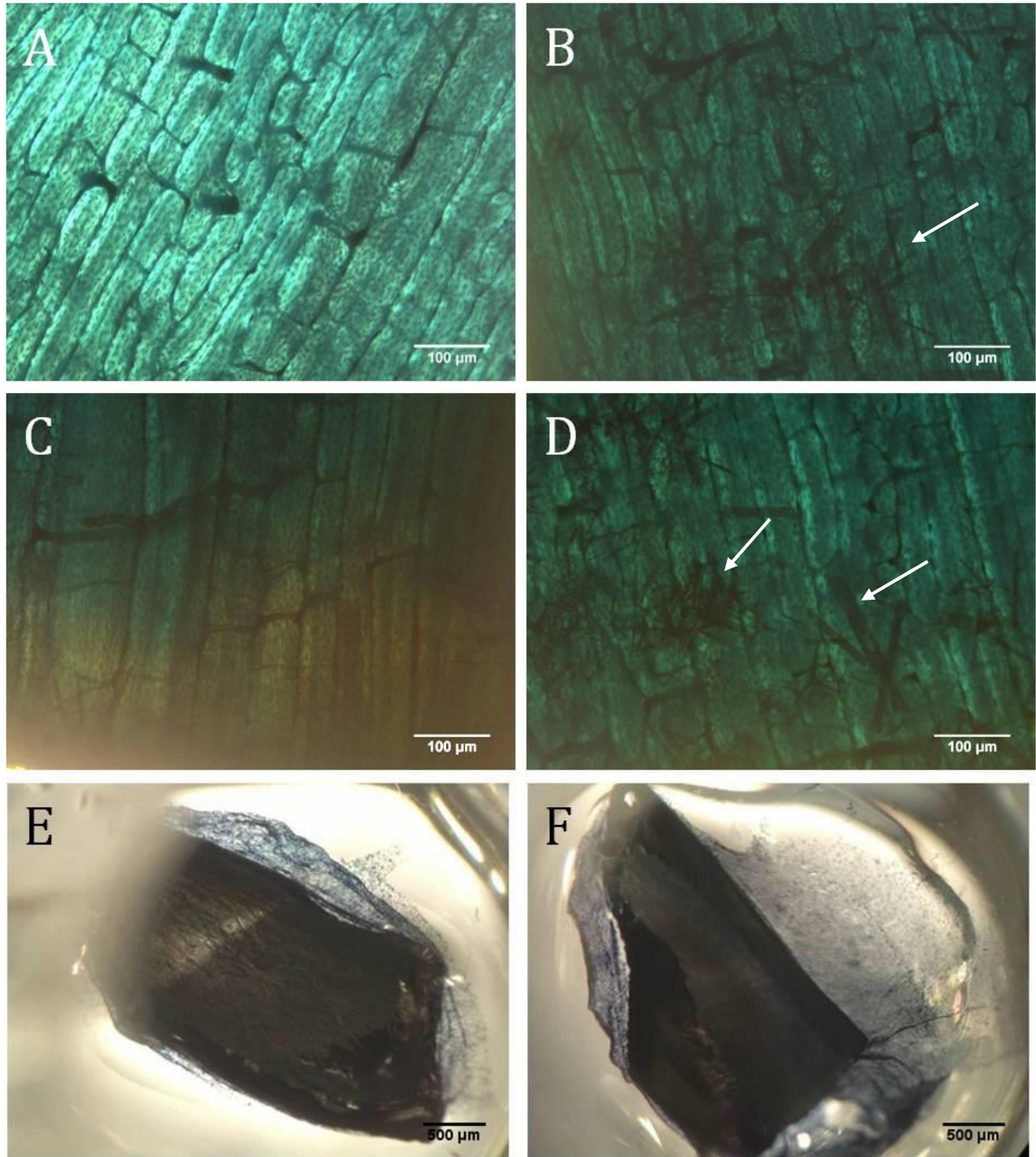


Figure 17. Representative bone pieces after demineralization treatment and staining with Goldner's trichrome. Mineralized matrix is visualized in green, partly or completely unmineralized matrix in yellow/red and cell nuclei and unspecific matrix in black. (A) The control bone piece lacking demineralization. (B) Bone piece with 6 hours of demineralization treatment. Unidentified structures were observed as unmineralized flakes on top of the mineralized bone matrix. (C) Bone piece with 48 hours of demineralization treatment. Expected demineralization process can be observed at the edge of the bone samples. (D) Bone piece with 48 hours of demineralization treatment with the flake structures still present. (E) Bone piece with 4 days of demineralization treatment. Severe demineralization was observed and migration of the seeded MC3T3-E1 cells from the unmineralized bone tissue to the underlying plastic. (F) Bone piece with 21 days of demineralization treatment. Increased degree of demineralization as well as MC3T3-E1 cell migration was observed.

4.9 Osteoblast proliferation on partly demineralized bone

Total levels of RNA were detected after 48 hours for the MC3T3-E1 cells seeded onto bone pieces with increasing degree of demineralization. Prior to RNA measurements the samples were transferred to a new well to ensure that the detected levels of RNA came solely from the bone pieces and not from the surrounding plastic. The results are presented in Figure 18 with the levels of total RNA in ng/ μ l and time of demineralization indicated. A statistically significant increase of about 30% was observed on the control bone piece lacking demineralization, compared to the general levels of RNA detected for the partly demineralized bone pieces. No statistically significant difference in total RNA was observed with increasing degree of demineralization.

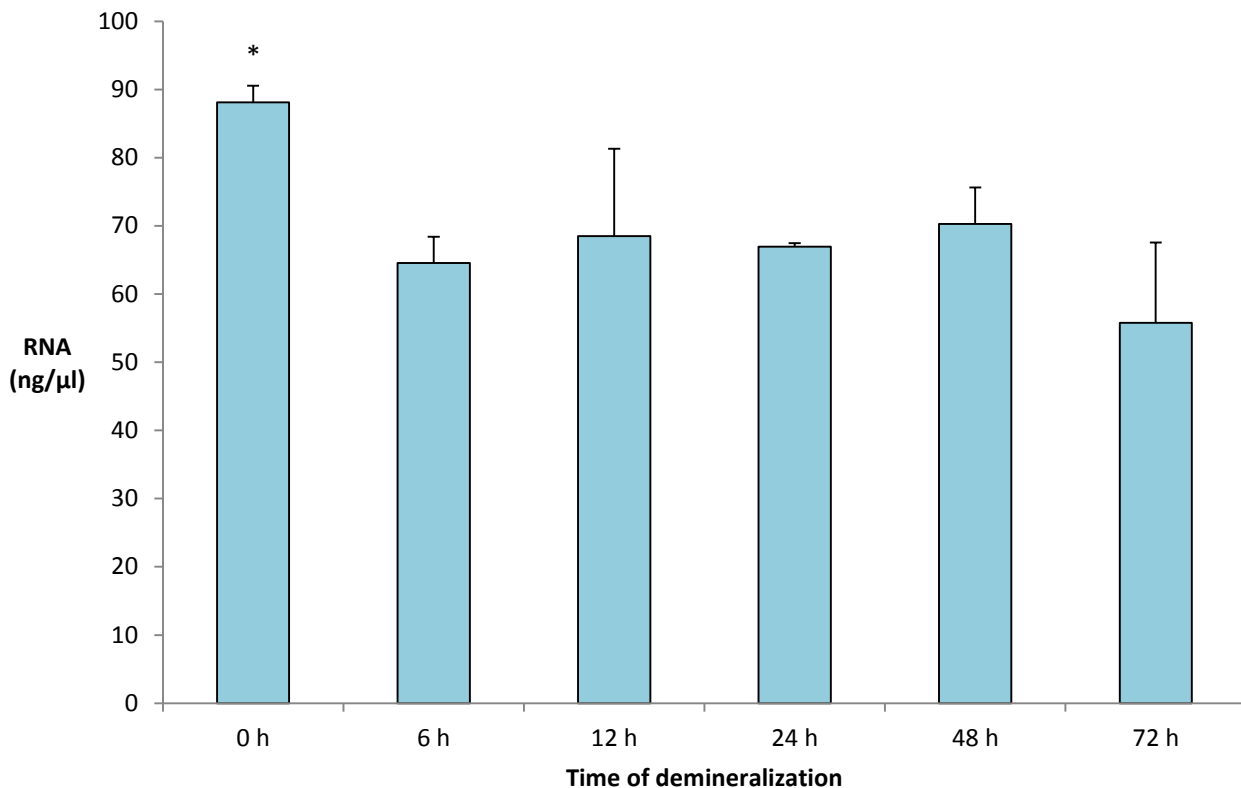


Figure 18. The measured RNA content in ng/ μ l for MC3T3-E1 cells seeded with concentration 5000 cells/cm² onto the control bone piece and partly demineralized bone pieces, with the demineralization time presented as hours from placement in EDTA. The RNA levels were measured after 48 hours of culture. Statistical significance is obtained between the control substrate (lacking demineralization) and the partly demineralized bone pieces.

The levels of total DNA of the MC3T3-E1 cells seeded onto the partly demineralized bone pieces were measured in the same samples as for RNA (see Figure 18) after 48 hours of culture. The results are presented in Figure 19 with the levels of total DNA in ng/ μ l and time of demineralization indicated. Significantly higher levels of total DNA was observed for the control bone piece lacking demineralization, which is in line with the detected levels of total RNA. The levels of total DNA observed on the control were about 50% higher than the levels detected on the demineralized bone samples. No significant difference in total DNA was observed between the different samples of demineralized bone pieces.

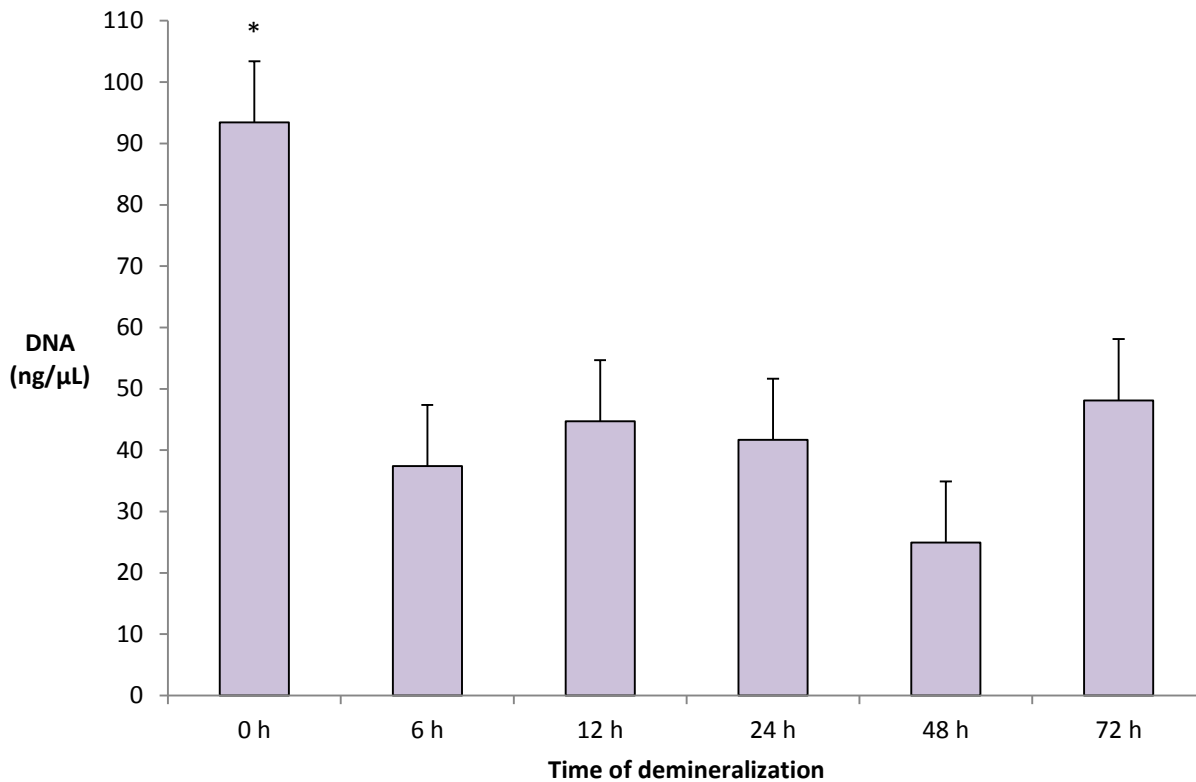


Figure 19. The measured levels of DNA presented in ng/ μ l for MC3T3-E1 cells seeded with concentration 5000 cells/cm² onto the control bone piece and partly demineralized bone pieces. The demineralization time is presented as hours from placement in EDTA and the DNA levels were measured after 48 hours of culture. One outlier has been removed from the samples at 72 hours. Statistical significance is obtained between the control substrate (lacking demineralization) and the partly demineralized bone pieces.

5. Discussion

5.1 Choice of substrates

The aim of this project was to determine how the stiffness of a culturing substrate affects different aspects of osteoblast development and activity. The microenvironment is known to influence a variety of cellular functions [49], which is particularly valid for bone cells since the skeletal remodelling process partly is coordinated by mechanical information. To evaluate the impact of substrate stiffness on seeded pre-osteoblast Mc3T3-E1 cells, polyacrylamide (PA) gels with three different stiffnesses were chosen as substrate. These three stiffnesses were chosen in the range of kPa to mimic different stages of relatively early osteoid mineralization. The chosen stiffnesses were a rough estimation since the precise mechanical properties of osteoid are unknown due to practical difficulties with *ex vivo* testing [44]. The substrate stiffnesses were, based on the mixing ratio of acrylamide and bisacrylamide during the production process, estimated to 4.8 kPa for the softest gel, 19 kPa for the medium gel and 77 kPa for the stiffest gel. The magnitude of these values were chosen based on documented finding that substrates with stiffness in the range of 20-40 kPa optimizes osteoblast differentiation [49]. Even if the exact stiffness of osteoid at different time points currently is impossible to establish is it most likely that osteoblasts *in vivo* experience osteoid stiffnesses in the range of the ones chosen in this project during some part of the bone remodelling process. This can be claimed since osteoid is secreted as a soft non-mineralized collagen matrix with low stiffness values, which is slowly mineralized into new bone with stiffness in the range of GPa. The fact that the estimated stiffnesses of the PA gels did not coincide with the measured stiffnesses (6.4 ± 0.7 kPa for the softest gel, 72.9 ± 1.7 kPa for the medium gel and 135.9 ± 3.4 kPa for the stiffest gel) was therefore not an obstacle, since the three stiffnesses still spanned a large stiffness range in the order of kPa.

The PA gels were further chosen as culturing substrates since they are widely accepted as effective means to tune ECM mechanics and have the main advantage of enable production of gels with diverse mechanical properties under identical conditions. In theory, this limits the differences between produced gels to solely mechanical properties. It has previously been proposed that hydrogels, such as PA gels, in general not possesses sufficient mechanical properties to provide cells with appropriate signals to mimic the complex *in vivo* environment [3]. However, Sire *et al.* reported in 2013 that primary osteoblasts are capable to develop a clear osteoblast morphology, express osteoblast associated proteins and mineralize the local ECM when cultured on dense collagen scaffolds, thereby supporting the claim that collagen scaffolds works as appropriate osteoid models *in vitro* [61]. In that study the osteoblasts were cultured on the surface of a 3D model and to what extent the collagen type I coating of the PA gels in this project is sufficient for the MC3T3-E1 cells to mimic *in vivo* conditions remains uncertain. However, the MC3T3-E1 cells in this project developed an elongated osteoblast-like morphology (see Figure 10) and expressed

osteoblast markers (see Figure 14). Further, the presence of ALP activity (see Figure 13) follows the expected patterns for mature osteoblasts and there is no reason to believe that the collagen type I coating of the PA gels affected the development of the MC3T3-E1 cells in an unexpected way.

To obtain a more accurate mimicking of the *in vivo* conditions for osteoblasts an alternative substrate was applied; demineralized cow bone. Since osteoid is unmineralized bone matrix, different degree of demineralized bone would represent different stages of the osteoid mineralization process *in vivo*. Demineralized bone is widely applied cell substrate in bone research due to its reported osteoinductive and osteoconductive properties. In addition, bone morphogenetic proteins naturally present during bone turnover are preserved in the demineralized bone and facilitate the regulation of MC3T3-E1 cell differentiation and function [62] [63]. There is however also drawbacks with the use of demineralized bone pieces as cellular substrate. Concerns have been made over the sterility process and even if demineralized bone powder previously successfully have been applied as MC3T3-E1 cell substrate [64], the experiments are not possible to reproduce. This is due to the fact that neither the concentration of collagen type I nor the structure of the bone matrix is exactly known and varies with respect to donor and skeleton region. It is also possible that the original composition of the bone matrix is modified during the demineralization process. This process is in turn very difficult to define since different degree of demineralized products may be absorbed in the remaining scaffold substrate and possibly interfere with the osteoblast maturation process and osteoid production. An approach with determine the actual stiffness of the demineralized bone pieces with indentation, in the same procedure as performed for the PA gel substrates, would have been desirable but unfortunately this was not possible during this project. Instead, the degree of demineralization was evaluated with Goldner's trichrome staining. This type of staining is usually applied to visualize distribution of different matrices and cell nuclei in connective tissues and the approach to visualize the degree of bone demineralization, as applied in this project, was a novel approach. It is therefore not possible to explain the presence of flake structures (see Figure 17) after demineralization treatments and staining from literature sources. The flakes were stained red, which indicates an unmineralized structure, and they could be the result of a reaction between remaining products from the demineralization treatment with EDTA and the Goldner's trichrome staining. This is supported by the fact that the flakes were observed on top of the mineralized bone surface, rather than as an integrated part of it, and that they only were observed on the bone pieces that had undergone EDTA treatment. After 48 hours the expected demineralization pattern from the EDTA treatment for the first time appeared at the edges of the bone pieces but it is likely that the EDTA treatment but results obtained for MC3T3-E1 cell proliferation on the different bone pieces (see Figure 18 and Figure 19) indicates that the EDTA treatment has affected the stiffness of the bone pieces already after 6 hours. After 4 days of

demineralization the bone pieces showed a deep dark colour after staining with Goldner's trichrome and it was no longer possible to distinguish any separate parts of the bone structure. This could be due to extensive red staining of a completely demineralized matrix but it can also not be excluded that the detected flake structures interfered with the demineralization process. The flakes were detected on top of the mineralized bone surface and it is possible that the flakes after 4 days completely are covering an underlying mineralized surface.

5.2 Effect of substrate stiffness on osteoblast activity

The influence of substrate stiffness on the ability of MC3T3-E1 cells to proliferate was evaluated by measure the levels of total RNA and DNA for cells seeded onto both the PA gel substrates and the partly demineralized bone pieces. In addition, attempts to measure levels of total proteins were conducted but the levels were too low to be detected. This was likely due to the cell number on the substrates after 48 hours of culture. For total RNA and DNA, significantly higher levels were detected for the cells seeded onto control bone pieces compared to the partly demineralized bone samples (see Figure 18 and Figure 19). The higher levels can be argued a result of an up-regulated proliferation, which would support the claim that stiffer bone samples enhance the maturation process of MC3T3-E1 cells, with detectable results within 48 hours of culture. The same trend could not be established for the MC3T3-E1 cells seeded onto the PA gels but there are several possible explanations for this. As mention in section 5.1, there are bone morphogenetic proteins present in the bone samples which enhance the maturation process of the pre-osteoblast MC3T3-E1 cells. It is therefore possible that any difference in proliferation was undetectable for the cells seeded onto the PA gels after 48 hours of culture, but that a difference would have been detected at a later time point. Another explanation for the higher degree of proliferation detected on the stiffer bone substrates is that stiffer substrates have a documented ability to support cell attachment, which was further proven for MC3T3-E1 cells on PA gels in this project (see Figure 10). There is no reason to believe that the same effect does not applied to bone samples of different stiffness and a higher cell number would then be expected on the control bone piece compared to the softer bone pieces that have undergone partly or complete demineralization. A higher cell number would as a natural result increase detected levels of total RNA and DNA and the fact that the effect cannot be detected for the MC3T3-E1 cells seeded onto the PA gels can once again be explained by the nature of bone pieces. This would mean that the same trend with higher degree of proliferation on stiffer substrates likely would have been detected also for the PA gels at a time point later than 48 hours.

The preference of stiffer bone samples was further observed in the second set of demineralized bone pieces, where an increased degree of MC3T3-E1 cell migration from

the bone piece to the underlying plastic of the well bottom was observed with an increased degree of bone demineralization (data shown for day 4 and 21 in Figure 17E and Figure 17F). More extensive demineralization results in a softer bone substrate, which further supports the claim that stiffer substrates induce MC3T3-E1 cell attachment. An attempt to confirm that the substrate stiffness also affect the metabolic activity of seeded cells was performed after 7 days of culture. The approach was to evaluate if the MC3T3-E1 cells were stimulated by mechanical cues from the substrate stiffness to secrete osteoid. Since collagen type I is the main component in osteoid a staining with Sirius Red to detect extracellular collagen type I was performed (see Figure 15). The fact that the PA gels had been coated with collagen type I increased explicable the risk of unspecific staining but it was considered an acceptable risk due to documented observations indicating that MC3T3-E1 cells are able to degrade the major part of their collagen type I matrix within 48 hours [65]. In that study the cells were stimulated by addition of vitamin D ($1,25(\text{OH})_2\text{D}_3$) but since the time point chosen in this project was considerable later it was still worth to evaluate if the effect with collagen type I degradation was the same. Coated PA gels with and without seeded MC3T3-E1 cells were therefore stained for collagen type I and compared. The results clearly showed that the seeded MC3T3-E1 cells had degraded their matrix after 7 days of culture also without addition of vitamin D. Instead of the red staining expected, the collagen type I coating in Figure 15F displayed a dark grey staining. The appearance of the grey staining indicated that it had been diminished due to extensive washing and the distinct red staining of collagen type I had instead remained protected inside the cell membrane of the MC3T3-E1 cells. No stained extracellular collagen type I indicating secreted osteoid was detected outside the membrane of the MC3T3-E1 cells. The possibility that also staining of secreted osteoid has been removed during washing steps cannot be excluded but it could also mean that no secretion of osteoid have taken place among the seeded osteoblasts. In other words, that osteoid has been produced by the seeded MC3T3-E1 cells but not yet been secreted into the ECM. It should however be noted that collagen type I is secreted by osteoblasts as monomers which assemble into collagen fibres in the ECM. Therefore it is more likely that the Sirius Red F3B dye has stained long fibres located inside the MC3T3-E1 cell membrane but that these not *per se* indicate the presence of collagen or unsecreted osteoid, but rather are a natural part of the intracellular matrix.

It would at least be expected that MC3T3-E1 cells stimulated with an addition of vitamin D secret osteoid after one week due to an enhanced differentiation but this was not the case. However, since staining with Sirius Red F3B is a qualitative evaluation method it is not possible to only based on these data confirm that no osteoid secretion has taken place after 7 days. Instead, quantitative evaluation techniques should be applied as addition to obtain a more nuanced picture of the impact of substrate stiffness on metabolic activity of osteoblast. Several quantitative alternatives exist to evaluate the ability of cells to synthesize collagen type I, where the most common methods includes detection of

procollagen type I N-terminal propeptide (PINP) in a sample, which is a natural product during the synthesis of collagen type I [66], and to measure the incorporation of [³H] – proline into collagenase-digestible proteins [67].

5.3 Substrate stiffness guide osteoblast differentiation

ALP activity functions as an early osteoblast marker and is commonly measured to examine the level of osteoblast differentiation. To evaluate the impact of substrate stiffness on MC3T3-E1 cell differentiation the levels of ALP activity were therefore detected after 24 hours, 48 hours and 7 days of culture. These time points were chosen to obtain an idea of how the stiffness of the substrates affected osteoblast differentiation over time. As seen in Figure 13A, the MC3T3-E1 cells are after 24 hours still growing at sub-confluent concentrations and ALP activity can only be detected on the stiffest PA gel and the plastic controls. The two later time points, presented in Figure 13B and Figure 13C, demonstrate that the ALP activity increase with time. This was the expected outcome since previous studies have observed a continuous increase in ALP activity for seeded MC3T3-E1 cells until 16 [47] and 18 [43] days of culture. Those studies used vitamin D to enhance the differentiation process and also in this study the highest levels of ALP activity was observed for the MC3T3-E1 cells cultured on plastic control substrates with an addition of vitamin D (PCD). This further supports the documented ability of vitamin D on MC3T3-E1 cell differentiation. The fact that no or very modest levels of ALP activity was observed on all substrates after 24 hours indicated however that the enhancing effect of vitamin D becomes more evident after 72 hours and 7 days of culture.

The fact that ALP activity was observed for MC3T3-E1 cells seeded on the stiffest PA gel and the plastic controls, but not for the softer PA gels, shows a clear difference in substrate ability to via mechanically induced signals stimulate differentiation. Higher degree of differentiation results in a down-regulated proliferation, which is supported by the fact that no difference in levels of total RNA (see Figure 11) and DNA (see Figure 12) was detected between the PA gels. However, the ALP activity indicated a modest difference in differentiation between 24 and 72 hours of culture and, as mention in section 5.2, the time point chosen for detection of proliferation for the PA gel substrates (48 hours) might be too soon to actually distinguish a difference in differentiation and proliferation between cells seeded on the PA gels. Both previous studies [44] [47] and results obtained in this project however establish beyond reasonable doubts that a stiffer culturing substrate enhance the maturation process among osteoblasts.

5.4 Impact of substrate stiffness on osteoblast gene expression

To evaluate the effect of osteoblast gene expression when cultured on the PA gels and plastic controls, five bone formation markers were detected with RT-PCR after 48 hours. No expression of osteocalcin or alkaline phosphatase (ALP) could be detected for MC3T3-

E1 cells seeded onto any of the substrates. This is not very surprising since both of these proteins are considered markers of mature osteoblasts and, like earlier discussed in sections 5.1 and 5.2, the PA gels applied in this project most likely are unable to induce a high degree of osteoblast differentiation after 48 hours. This statement is supported by results obtained by Putnam *et al.* in 2007 [68], who detected a substrate dependent expression pattern of several bone formation markers in MC3T3-E1 cells, but only after 7 days of culture. The theory that 48 hours is too early to detect a difference in gene expression between the PA gel substrates applied in this project is also supported by the fact that collagen type I, osteopontin and bone sialoprotein were detected. These three markers are namely expressed earlier than ALP and osteocalcin in the osteoblast maturation process.

A trend with higher expression of collagen type I, osteopontin and bone sialoprotein was observed on the plastic controls (see Figure 14) but no enhancing effect of vitamin D could be distinguished between PC and PCD, which is supported by the detected levels of MC3T3-E1 cell differentiation on these two substrates (see Figure 13). The fact that no significant difference was observed in gene expression between the PA gel substrates with different stiffness is surprising due to the documented ability of stiffer substrates to enhance osteoblast differentiation. This could, as previously discussed in sections 5.1 and 5.2, be due to the time point chosen but it should also be noted that the markers were detected in a late run of the RT-PCR (36), which indicated low amounts of initial cDNA and might interfere with the quantification process. It is further questionable however the expression of osteopontin actually indicates the formation of osteoid. Osteopontin has a wide range of biological applications for osteoblasts in addition to bone formation. When associated with bone formation, osteopontin is usually expressed later than ALP, which in turn is stimulated by the osteoblast transcription factor Runx2. Thus, the fact that osteopontin but no ALP was detected implies that the osteopontin detected might have another function than part of the bone formation process. It can however be established beyond doubt that all the PA gels and plastic controls induce appropriate mechanical signals to induce differentiation of the pre-osteoblast MC3T3-E1 cells within 48 hours of culture.

5.5 Osteoblast induced mineralization of ECM

One major function of mature osteoblasts consists of mineralizing the secreted bone. Therefore, to evaluate the impact of substrate stiffness on this function the presence of calcium nodules were evaluated on the PA gel substrates and plastic. This was done by performing a staining with Alizarin Red S, which is a well-established method to detect the presence of matrix mineralization. No calcium nodules could be detected after 13 days of MC3T3-E1 cell culture, with exception of the plastic control treated with vitamin D (see Figure 16). This was an expected outcome considering the fact that vitamin D induces

differentiation among MC3T3-E1 cells, as observed in this project (see Figure 13) and reported in previous studies [45] [47], and as a natural result therefore also speeds up the bone mineralization process. In addition to the calcium nodules detected among the osteoblasts seeded onto the PCD samples, extensive unspecific staining of Alizarin Red S was observed in deeper cell layers (data not shown). The phenomena with accumulated Alizarin Red S staining within thicker layers of cell culture has previously been observed [40] [69] but the culture medium applied in those projects was enriched with additional inorganic phosphor to enhance the mineralization process. Inconclusive results with Alizarin Red S staining have been reported in several studies [70] [71], which not only shows limitations with the detection method but also indicates difficulties in inducing matrix mineralization of MC3T3-E1 cells *in vitro*. Most studies report a minimum culture time of two weeks for MC3T3-E1 cells before any calcium nodules can be detected but others report observation of matrix mineralization after significantly shorter time of culture than used in this project, and even as early as from day 4 [44]. This reported inconsistency can only partly be explained by the inequality in Alizarin Red S staining procedures. Rather, it is likely a result of several factors combined, such as MC3T3-E1 culture conditions, cell seeding concentration, composition of the culture medium, substrate properties and cell passage number used. Chung *et al.* observed in 1999 that MC3T3-E1 cells undergoes a drastic change in cell morphology and function between early and late passages [72] and Yan *et al.* reported further in 2013 a dramatic decrease in matrix mineralization for increasing cell passage number [73].

A higher initial cell seeding concentration (10 000 cells/cm²) was applied in these experiments compared to the others (5000 cells/cm²) conducting during this project. This was done to shorten the proliferation time and thereby accelerating the differentiation and bone mineralization process. The reason for not applying an even higher initial cell seeding concentration or extend the experimental period beyond 13 days was the risk of cell detachment, which often is the case when MC3T3-E1 cells are cultured *in vitro* until they comprise more than a monolayer. However, several factors impact the behaviour of the MC3T3-E1 cells in culture and in a study conducted by Moran *et al.* in 1998 [40] an initial MC3T3-E1 cell seeding concentration of 50 000 cells/cm² was applied without detectable matrix mineralization after 31 days of culture. The initial cell seeding concentration has also previously been shown to play a subordinate role in the time preceding matrix mineralization [44] and it is likely that the solution to the problem with osteoblast detachment *in vitro* instead much be searched elsewhere. One possible solution would be to tune the properties of the culturing model. This was done in a study by Giraud-Guille in 2013 [61], where matrix mineralization by primary human pre-osteoblasts could be studied until 60 days of culture with the use of a 3D culture model. These type of models increased cell attachment and provide a better mimicking of *in vivo* conditions but also introduced more problems in evaluating the results compared to conventional 2D culture models.

6. Conclusions

There are a number of limitations in this project but the results obtained clearly demonstrate the importance of the mechanical properties of the ECM on osteogenic maturation and MC3T3-E1 cells number. Stiffer substrates were shown to induce higher degree of cell attachment among the osteoblasts and higher levels of differentiation and proliferation were clearly associated with the stiffer culturing substrates.

The substrate stiffness has therefore been proven to affect osteoblast development and behaviour, but no impact of substrate stiffness on metabolic activity could be identified in this project. This indicates that the osteoid production by osteoblasts might be influenced by several aspects and not is a direct result of the culture substrate stiffness.

7. Future prospective

In this project, the osteoblasts were shown to be affected by the mechanical properties of the culturing substrates but the role of mechanotransduction during the formation of the lamellar structure in cortical bone *in vivo* remains more uncertain. To further evaluate the theory that osteoblasts preferably produce osteoid on a stiffer substrate is it crucial to be able to measure the levels of total protein produced by MC3T3-E1 cells cultured onto the different sample stiffnesses. In this project the levels were too low to be detected after 48 hours of MC3T3-E1 cell culture. This problem can however be avoided by either increasing the cell seeding number, extend the time of cell culture or produce larger PA gels. The two former options are not ideal consider the tendency of the MC3T3-E1 cells to detach from the surface when the culture time is prolonged beyond the point of confluence. The latter one is on the other hand a suitable next step since larger PA gels would enable the same cell seeding number (cells/cm²) and culture time and still ensure higher levels of total protein produced on the different substrates due to an increased total cell number. It is further desirable in future experiments to apply negative controls, such as a cell type known to not produce osteoid (*i.e.* fibroblasts) seeded onto all PA gel stiffnesses. This would enable a superior control of the osteoblast phenotype and identify possible trans-differentiation of the osteoblast into another cell type with mesenchymal stem cell origin during the project. Another approach is to use primary osteoblasts instead of the cell line MC3T3-E1 cells, since these cells reflect properties of osteoblasts *in vivo* better than an osteoblast cell line. Even though the MC3T3-E1 cells line is established as a good model system *in vitro* is it still possible that the primary osteoblasts react different than the MC3T3-E1 cells on the mechanical properties of the substrates.

A difference in proliferation based on levels of total RNA and DNA was observed for the MC3T3-E1 cells seeded onto the control bone piece lacking demineralization compared to the partly demineralized bone pieces. However, this effect cannot be concluded a result of the substrate stiffness since it was not possible to determine exact stiffness of the bone pieces after demineralization treatment. It is however worth further investigation and a first step is to determine the exact stiffness of the resulting bone pieces. This would preferably be performed with indentation using a probe more suitable for stiffer substrates, since the bone pieces are assumed to have stiffnesses far above the PA gels also after demineralization treatment. It would be interesting to see if the difference in proliferation was also detectable for the levels of total protein. These levels were however also in this case below the limit of detection but the same solution as for the PA gels is desirable since larger bone pieces also in this case would increase the cell number and as a result increase the levels of total protein. Taken together few conclusions can be drawn solely from the obtained data in this project but the results are promising for further research.

8. References

- [1] Carnelli, D., P. Vena, M. Dao, C. Ortiz, and R. Contro (2013) Orientation and size-dependent mechanical modulation within individual secondary osteons in cortical bone tissue. *Journal of the Royal Society Interface*. 10.
- [2] Thompson, W. R., C. T. Rubin, and J. Rubin (2012) Mechanical regulation of signaling pathways in bone. *Gene*. 503: 179-193.
- [3] Discher, D. E., P. Janmey, and Y. L. Wang (2005) Tissue cells feel and respond to the stiffness of their substrate. *Science*. 310: 1139-1143.
- [4] Reisinger, A. G., D. H. Pahr, and P. K. Zysset (2011) Elastic anisotropy of bone lamellae as a function of fibril orientation pattern. *Biomechanics and Modeling in Mechanobiology*. 10: 67-77.
- [5] Cowin, S. C., and D. H. Hegedus (1976) BONE REMODELING .1. THEORY OF ADAPTIVE ELASTICITY. *Journal of Elasticity*. 6: 313-326.
- [6] Doblare, M., J. M. Garcia, and M. J. Gomez (2004) Modelling bone tissue fracture and healing: a review. *Engineering Fracture Mechanics*. 71: 1809-1840.
- [7] Wagermaier, W., H. S. Gupta, A. Gourrier, M. Burghammer, P. Roschger, and P. Fratzl (2006) Spiral twisting of fiber orientation inside bone lamellae. *Biointerphases*. 1: 1-5.
- [8] Weiner, S., W. Traub, and H. D. Wagner (1999) Lamellar bone: Structure-function relations. *Journal of Structural Biology*. 126: 241-255.
- [9] Enlow, D. H. (1962) FUNCTIONS OF HAVERSIAN SYSTEM. *American Journal of Anatomy*. 110: 269-&.
- [10] Marotti, G., M. Ferretti, and C. Palumbo (2013) The problem of bone lamellation: An attempt to explain different proposed models. *Journal of Morphology*. 274: 543-550.
- [11] Giraudguille, M. M. (1988) TWISTED PLYWOOD ARCHITECTURE OF COLLAGEN FIBRILS IN HUMAN COMPACT-BONE OSTEOONS. *Calcified Tissue International*. 42: 167-180.
- [12] Weiner, S., T. Arad, I. Sabanay, and W. Traub (1997) Rotated plywood structure of primary lamellar bone in the rat: Orientations of the collagen fibril arrays. *Bone*. 20: 509-514.
- [13] Ruth, E. B. (1947) BONE STUDIES .1. FIBRILLAR STRUCTURE OF ADULT HUMAN BONE. *American Journal of Anatomy*. 80: 35-53.
- [14] Marotti, G., and M. A. Muglia (1988) A scanning electron microscope study of human bony lamellae. Proposal for a new model of collagen lamellar organization. *Archivio italiano di anatomia e di embriologia. Italian journal of anatomy and embryology*. 93: 163-175.
- [15] Yamamoto, T., T. Hasegawa, M. Sasaki, H. Hongo, C. Tabata, Z. Liu, M. Li, and N. Amizuka (2012) Structure and formation of the twisted plywood pattern of collagen fibrils in rat lamellar bone. *Journal of Electron Microscopy*. 61: 113-121.
- [16] Faingold, A., S. R. Cohen, and H. D. Wagner (2012) Nanoindentation of osteonal bone lamellae. *Journal of the Mechanical Behavior of Biomedical Materials*. 9: 198-206.
- [17] Varga, P., A. Pacureanu, M. Langer, H. Suhonen, B. Hesse, Q. Grimal, P. Cloetens, K. Raum, and F. Peyrin (2013) Investigation of the three-dimensional orientation of mineralized collagen fibrils in human lamellar bone using synchrotron X-ray phase nano-tomography. *Acta Biomaterialia*. 9: 8118-8127.
- [18] Marotti, G. (1996) The structure of bone tissues and the cellular control of their deposition. *Italian journal of anatomy and embryology = Archivio italiano di anatomia ed embriologia*. 101: 25-79.
- [19] Ducy, P., T. Schinke, and G. Karsenty (2000) The osteoblast: A sophisticated fibroblast under central surveillance. *Science*. 289: 1501-1504.
- [20] Everts, V., J. M. Delaisse, W. Korper, D. C. Jansen, W. Tigchelaar-Gutter, P. Saftig, and W. Beertsen (2002) The bone lining cell: Its role in cleaning Howship's lacunae and initiating bone formation. *Journal of Bone and Mineral Research*. 17: 77-90.

- [21] Dierkes, C., M. Kreisel, A. Schulz, J. Steinmeyer, J. C. Wolff, and L. Fink (2009) Catabolic Properties of Microdissected Human Endosteal Bone Lining Cells. *Calcified Tissue International*. 84: 146-155.
- [22] Dallas, S. L., and L. F. Bonewald (2010) Dynamics of the transition from osteoblast to osteocyte. *Skeletal Biology and Medicine*. 1192: 437-443.
- [23] Teitelbaum, S. L. (2000) Bone resorption by osteoclasts. *Science*. 289: 1504-1508.
- [24] Deng, J., B. E. Petersen, D. A. Steindler, M. L. Jorgensen, and E. D. Laywell (2006) Mesenchymal stem cells spontaneously express neural proteins in culture and are neurogenic after transplantation. *Stem Cells*. 24: 1054-1064.
- [25] Pittenger, M. F., A. M. Mackay, S. C. Beck, R. K. Jaiswal, R. Douglas, J. D. Mosca, M. A. Moorman, D. W. Simonetti, S. Craig, and D. R. Marshak (1999) Multilineage potential of adult human mesenchymal stem cells. *Science*. 284: 143-147.
- [26] McBeath, R., D. M. Pirone, C. M. Nelson, K. Bhadriraju, and C. S. Chen (2004) Cell shape, cytoskeletal tension, and RhoA regulate stem cell lineage commitment. *Developmental Cell*. 6: 483-495.
- [27] Kreke, M. R., W. R. Huckle, and A. S. Goldstein (2005) Fluid flow stimulates expression of osteopontin and bone sialoprotein by bone marrow stromal cells in a temporally dependent manner. *Bone*. 36: 1047-1055.
- [28] Li, Y. J., N. N. Batra, L. D. You, S. C. Meier, I. A. Coe, C. E. Yellowley, and C. R. Jacobs (2004) Oscillatory fluid flow affects human marrow stromal cell proliferation and differentiation. *Journal of Orthopaedic Research*. 22: 1283-1289.
- [29] Papachroni, K. K., D. N. Karatzas, K. A. Papavassiliou, E. K. Basdra, and A. G. Papavassiliou (2009) Mechanotransduction in osteoblast regulation and bone disease. *Trends in Molecular Medicine*. 15: 208-216.
- [30] Watt, F. M., and W. T. S. Huck (2013) Role of the extracellular matrix in regulating stem cell fate. *Nature Reviews Molecular Cell Biology*. 14: 467-473.
- [31] Christenson, R. H. (1997) Biochemical markers of bone metabolism: An overview. *Clinical Biochemistry*. 30: 573-593.
- [32] Tan, S. D., T. J. de Vries, A. M. Kuijpers-Jagtman, C. M. Semeins, V. Elverts, and J. Klein-Nulend (2007) Osteocytes subjected to fluid flow inhibit osteoclast formation and bone resorption. *Bone*. 41: 745-751.
- [33] Miller, S. C. (1987) THE BONE LINING CELL - A DISTINCT PHENOTYPE. *Calcified Tissue International*. 41: 1-5.
- [34] Parfitt, A. M., G. R. Mundy, G. D. Roodman, D. E. Hughes, and B. F. Boyce (1996) A new model for the regulation of bone resorption, with particular reference to the effects of bisphosphonates. *Journal of Bone and Mineral Research*. 11: 150-159.
- [35] Raggatt, L. J., and N. C. Partridge (2010) Cellular and Molecular Mechanisms of Bone Remodeling. *Journal of Biological Chemistry*. 285: 25103-25108.
- [36] Boyle, W. J., W. S. Simonet, and D. L. Lacey (2003) Osteoclast differentiation and activation. *Nature*. 423: 337-342.
- [37] Zhou, H. Y., H. Takita, R. Fujisawa, M. Mizuno, and Y. Kuboki (1995) STIMULATION BY BONE SIALOPROTEIN OF CALCIFICATION IN OSTEOBLAST-LIKE MC3T3-E1 CELLS. *Calcified Tissue International*. 56: 403-407.
- [38] Ganss, B., R. H. Kim, and J. Sodek (1999) Bone sialoprotein. *Critical Reviews in Oral Biology & Medicine*. 10: 79-98.
- [39] Shi, S. T., M. Kirk, and A. J. Kahn (1996) The role of type I collagen in the regulation of the osteoblast phenotype. *Journal of Bone and Mineral Research*. 11: 1139-1145.
- [40] Beck, G. R., E. C. Sullivan, E. Moran, and B. Zerler (1998) Relationship between alkaline phosphatase levels, osteopontin expression, and mineralization in differentiating MC3T3-E1 osteoblasts. *Journal of Cellular Biochemistry*. 68: 269-280.

- [41] Rittling, S. R., H. N. Matsumoto, M. D. McKee, A. Nanci, X. R. An, K. E. Novick, A. J. Kowalski, M. Noda, and D. T. Denhardt (1998) Mice lacking osteopontin show normal development and bone structure but display altered osteoclast formation in vitro. *Journal of Bone and Mineral Research*. 13: 1101-1111.
- [42] Linez-Bataillon, P., F. Monchau, M. Bigerelle, and H. F. Hildebrand (2002) In vitro MC3T3 osteoblast adhesion with respect to surface roughness of Ti6Al4V substrates. *Biomolecular Engineering*. 19: 133-141.
- [43] Hoemann, C. D., H. El-Gabalawy, and M. D. McKee (2009) In vitro osteogenesis assays: Influence of the primary cell source on alkaline phosphatase activity and mineralization. *Pathologie Biologie*. 57: 318-323.
- [44] McNamara, L., C. Mullen, M. Haugh, M. Schaffler, and R. Majeska (2013) Osteocyte differentiation is regulated by extracellular matrix stiffness and intercellular separation. pp. 183-194 In: Editor (ed.)[^](eds.)]. *Book Title*. Publisher|, City|.
- [45] Willems, H. M. E., E. van den Heuvel, G. Carmeliet, A. Schaafsma, J. Klein-Nulend, and A. D. Bakker (2012) VDR dependent and independent effects of 1,25-dihydroxyvitamin D-3 on nitric oxide production by osteoblasts. *Steroids*. 77: 126-131.
- [46] Jorgensen, N. R., Z. Henriksen, O. H. Sorensen, and R. Civitelli (2004) Dexamethasone, BMP-2, and 1,25-dihydroxyvitamin D enhance a more differentiated osteoblast phenotype: validation of an in vitro model for human bone marrow-derived primary osteoblasts. *Steroids*. 69: 219-226.
- [47] Matsumoto, T., C. Igarashi, Y. Takeuchi, S. Harada, T. Kikuchi, H. Yamato, and E. Ogata (1991) STIMULATION BY 1,25-DIHYDROXYVITAMIN-D3 OF INVITRO MINERALIZATION INDUCED BY OSTEOBLAST-LIKE MC3T3-E1 CELLS. *Bone*. 12: 27-32.
- [48] Blattler, D. P., A. Bradley, K. Vanslyke, and F. Garner (1972) QUANTITATIVE ELECTROPHORESIS IN POLYACRYLAMIDE GELS OF 2-40 PERCENT. *Journal of Chromatography*. 64: 147-&.
- [49] Discher, D. E., L. Sweeney, S. Sen, and A. Engler (2007) Matrix elasticity directs stem cell lineage specification. *Biophysical Journal*. 32A-32A.
- [50] Chen, J. L., C. Burger, C. V. Krishnan, B. Chu, B. S. Hsiao, and M. J. Glimcher (2005) In vitro mineralization of collagen in demineralized fish bone. *Macromolecular Chemistry and Physics*. 206: 43-51.
- [51] Seo, S. B., A. Zhang, H. Y. Kim, J. A. Yi, H. Y. Lee, D. H. Shin, and S. D. Lee (2010) Technical Note: Efficiency of Total Demineralization and Ion-Exchange Column for DNA Extraction from Bone. *American Journal of Physical Anthropology*. 141: 158-162.
- [52] Johnson, K. (1970) The correlation of indentation experiments. pp. 115-126 In: Editor (ed.)[^](eds.)]. *Book Title*. Publisher|, City|.
- [53] VanLandingham, M. R. (2003) Review of instrumented indentation. *Journal of Research of the National Institute of Standards and Technology*. 108: 249-265.
- [54] Shiao, Y. H. (2003) A new reverse transcription-polymerase chain reaction method for accurate quantification. *Bmc Biotechnology*. 3.
- [55] Freeman, W. M., S. J. Walker, and K. E. Vrana (1999) Quantitative RT-PCR: Pitfalls and potential. *Biotechniques*. 26: 112-+.
- [56] Jekely, G., and D. Arendt (2007) Cellular resolution expression profiling using confocal detection of NBT/BCIP precipitate by reflection microscopy. *Biotechniques*. 42: 751-755.
- [57] Malkusch, W., B. Rehn, and J. Bruch (1995) ADVANTAGES OF SIRIUS-RED STAINING FOR QUANTITATIVE MORPHOMETRIC COLLAGEN MEASUREMENTS IN LUNGS. *Experimental Lung Research*. 21: 67-77.
- [58] Ichikawa, T., K. Horie-Inoue, K. Ikeda, B. Blumberg, and S. Inoue (2006) Steroid and xenobiotic receptor SXR mediates vitamin K-2-activated transcription of extracellular

- matrix-related genes and collagen accumulation in osteoblastic cells. *Journal of Biological Chemistry*. 281: 16927-16934.
- [59] Malluche, H. H., W. Meyer, D. Sherman, and S. G. Massry (1982) QUANTITATIVE BONE-HISTOLOGY IN 84 NORMAL AMERICAN SUBJECTS - MICRO-MORPHOMETRIC ANALYSIS AND EVALUATION OF VARIANCE IN ILIAC BONE. *Calcified Tissue International*. 34: 449-455.
- [60] Puchtler, H., S. N. Meloan, and M. S. Terry (1969) ON HISTORY AND MECHANISM OF ALIZARIN AND ALIZARIN RED S STAINS FOR CALCIUM. *Journal of Histochemistry & Cytochemistry*. 17: 110-&.
- [61] Silvent, J., N. Nassif, C. Helary, T. Azais, J.-Y. Sire, and M. M. G. Guille (2013) Collagen Osteoid-Like Model Allows Kinetic Gene Expression Studies of Non-Collagenous Proteins in Relation with Mineral Development to Understand Bone Biomineralization. *Plos One*. 8.
- [62] Kanzaki, S., W. Ariyoshi, T. Takahashi, T. Okinaga, T. Kaneuji, S. Mitsugi, K. Nakashima, T. Tsujisawa, and T. Nishihara (2011) Dual effects of heparin on BMP-2-induced osteogenic activity in MC3T3-E1 cells. *Pharmacological Reports*. 63: 1222-1230.
- [63] Groeneveld, E. H. J., and E. H. Burger (2000) Bone morphogenetic proteins in human bone regeneration. *European Journal of Endocrinology*. 142: 9-21.
- [64] Behnam, K., S. S. Murray, J. P. Whitelegge, and E. J. Brochmann (2002) Identification of the molecular chaperone alpha B-crystallin in demineralized bone powder and osteoblast-like cells. *Journal of Orthopaedic Research*. 20: 1190-1196.
- [65] Thomson, B. M., S. J. Atkinson, A. M. McGarrity, R. M. Hembry, J. J. Reynolds, and M. C. Meikle (1989) TYPE-I COLLAGEN DEGRADATION BY MOUSE CALVARIAL OSTEOBLASTS STIMULATED WITH 1,25-DIHYDROXYVITAMIN-D-3 - EVIDENCE FOR A PLASMINOGEN-PLASMIN-METALLOPROTEINASE ACTIVATION CASCADE. *Biochimica Et Biophysica Acta*. 1014: 125-132.
- [66] Koizumi, M., J. Yonese, I. Fukui, and E. Ogata (2001) The serum level of the amino-terminal propeptide of type I procollagen is a sensitive marker for prostate cancer metastasis to bone. *Bju International*. 87: 348-351.
- [67] Takuwa, Y., C. Ohse, E. A. Wang, J. M. Wozney, and K. Yamashita (1991) BONE MORPHOGENETIC PROTEIN-2 STIMULATES ALKALINE-PHOSPHATASE ACTIVITY AND COLLAGEN-SYNTHESIS IN CULTURED OSTEOBLASTIC CELLS, MC3T3-E1. *Biochemical and Biophysical Research Communications*. 174: 96-101.
- [68] Khatiwala, C. B., S. R. Peyton, M. Metzke, and A. J. Putnam (2007) The regulation of osteogenesis by ECM rigidity in MC3T3-E1 cells requires MAPK activation. *Journal of Cellular Physiology*. 211: 661-672.
- [69] Chung, C. H., E. E. Golub, E. Forbes, T. Tokuoka, and I. M. Shapiro (1992) MECHANISM OF ACTION OF BETA-GLYCEROPHOSPHATE ON BONE CELL MINERALIZATION. *Calcified Tissue International*. 51: 305-311.
- [70] Boskey, A. L. (1998) Biomineralization: Conflicts, challenges, and opportunities. *Journal of Cellular Biochemistry*. 83-91.
- [71] Boskey, A. L., S. B. Doty, D. Stiner, and I. Binderman (1996) Viable cells are a requirement for in vitro cartilage calcification. *Calcified Tissue International*. 58: 177-185.
- [72] Chung, C. Y., A. Iida-Klein, L. E. Wyatt, G. H. Rudkin, K. Ishida, D. T. Yamaguchi, and T. A. Miller (1999) Serial passage of MC3T3-E1 cells alters osteoblastic function and responsiveness to transforming growth factor-beta 1 and bone morphogenetic protein-2. *Biochemical and Biophysical Research Communications*. 265: 246-251.
- [73] X. Yan, W. Y., F. Yang, M. Kersten-Niessen (2013) Effects of Continuous Passaging on Mineralization of MC3T3-E1 Cells with Improved Osteogenic Culture Protocol. *TISSUE ENGINEERING*.

Appendix A

A.1 MC3T3-E1 medium, passaging and seeding

Reagents

- Cell culture medium (α -MEM supplemented with 10% fetal bovine serum (FBS), 1% vitamin C, 1% L-glutamine, 0.5% fungizone, 0.25% penicillin and 0.25% streptomycin)
- Phosphor Buffered Saline (PBS)
- Trypsin

Protocol

Medium for MC3T3-E1 cell culture

1. Mix the following medium components in a tube (final volume 10 ml):

α -MEM	8.7	(ml)
FBS	1	(ml)
Fungizone	50	(μ l)
Penicillin	25	(μ l)
Streptomycin	25	(μ l)
Vitamin C	100	(μ l)
L-glutamine	100	(μ l)

2. Filter the medium.
3. Mix by gently turn the tube repeatedly.

MC3T3-E1 cell passaging

1. Start the laminar flow hood, wait until the correct conditions are established and clean the working space with ethanol.
2. Make sure that enough MC3T3-E1 culture medium is present.
3. Remove the cells from the incubator and observe them with the microscope.
4. Place the cell culture flask in the laminar flow hood.
5. Remove the medium from the cell culture flask with a Pasteur pipette.

6. Carefully add PBS (10 ml for a T75 cm² flask or 20 ml for a T175 cm² flask).
7. Gently tilt the flask to wash away remaining medium and remove the PBS using a Pasteur pipette.
8. Add Trypsin (1 ml for a T75 cm² flask or 2 ml for a T175 cm² flask) and make sure that the flask surface is completely covered.
9. Incubate the flask for 10 minutes at 37°C and 5% CO₂.
10. Inspect the cells with the microscope and gently shake the flask if necessary for further detachment.
11. Deactivate the Trypsin by adding MC3T3-E1 culture medium (3 ml for a T75 cm² flask or 6 ml for a T175 cm² flask)
12. Pipette the cell solution up and down and transfer the solution to a 10 ml tube.
13. Centrifuge the solution for 10 minutes at 600 rpm in room temperature.
14. Discard the supernatant and detach the cells in the pellet.
15. Add MC3T3-E1 culture medium (1 ml for T75 cm² or 2 ml for T175 cm²).
16. Count the cells using the Muse™ Count & Viability Kit, according to manufacturer's protocol.
17. Label two new cell culture flasks and add MC3T3-E1 culture medium to each (20 ml for a T75 cm² flask or 40 ml for a T175 cm² flask).
18. Add the calculated amount of cell solution into each of the two new cell culture flasks.
19. Gently tilt the cell culture flasks to ensure an even cell distribution.
20. Make sure that the opening of the cell culture flask is completely dry before placing the flask in the incubator at 37°C and 5% CO₂.

MC3T3-E1 cell seeding

1. Obtain the cell solution according to protocol "MC3T3-E1 cell passaging".
2. Count the cells in the sample using the Muse™ Count & Viability Kit, according to manufacturer's protocol, with dilution factor 20.
3. Add MC3T3-E1 culture medium to obtain the desired cell density.
4. Mix the cell solution regularly during the cell seeding procedure to ensure equal cell density in wells.
5. Pipette the calculated amount of cell solution into each well.
6. Place the plate in the incubator at 37°C and 5% CO₂.

A.2 Process of bone demineralization

Reagents

- EDTA (4.2%, pH 7.0)
- Distilled water
- Phosphor Buffered Saline (PBS)
- Antibiotic antimycotic solution

Protocol

1. Make EDTA (4.2%, pH 7.0) solution:
 - Add 4.2 g of EDTA powder to 90 ml distilled water.
 - Mix gently and measure continuously pH.
2. Put the bone pieces in the wells of a 96-well plate.
3. Add the EDTA solution to the bone pieces that will be demineralized and PBS to the control bone pieces.
4. Add 250 μ l Antibiotic antimycotic solution to each well.
5. Every 3-4 day refresh the EDTA solution and replace the EDTA with PBS for two of the wells.

A.3 Production of polyacrylamide (PA) gel substrates

Reagents

- Phosphor Buffered Saline (PBS)
- Acetone
- Silane (3-(Trimethoxysilyl)propylmethacrylate)
- Gel stock solution
- Ammonium persulfat (10%)
- Distilled water

Protocol

1. Put the cover glasses in a beaker containing 25 ml acetone and 100 μ l silane (3-(Trimethoxysilyl)propylmethacrylate).
2. Let the beaker incubate for 20 minutes under gently shaking.
3. Remove the cover glasses carefully to a beaker containing 25 ml pure acetone.
4. Let the beaker incubate for 10 minutes under gently shaking.
5. Place the cover glasses in a tube with PBS and store in fridge until use.

6. Mark four tubes with soft (estimated to 4.8 kPa), medium (estimated to 19 kPa) and stiff (estimated to 77 kPa).
7. Make the gel stock solutions by mixing the components (in μ l) below:

Estimated stiffness (kPa)	Soft (4.8)	Medium (19)	Stiff (77)
Distilled water	684	593	478
TEMED	1.5	1.5	1.5
40% Acrylamide	187.5	187.5	300
2% Bisacrylamide	27	118	120.5
<i>Total</i>	900	900	900

8. Add 20 μ l ammonium persulfat (APS) 10% into a tube.
9. Add 180 μ l of the gel stock solution.
10. Quickly mix by using the pipette.
11. Quickly place 4 to 5 drops of 20 μ l solution each on glass plate.
12. Quickly place glass cover slips on top.
13. Let polymerize for about 1 minute.
14. Remove cover slips with attach gel to 12-well plate.
15. Add 1 ml distilled water to each well and gel.
16. Keep in fridge until use.

A.4 Application of coating

Reagents

- Phosphor Buffered Saline (PBS)
- Antibiotic antimycotic solution
- Sulfo-SANPAH (100 mM)
- HEPES (50 mM)
- Collagen type I rat tail (5 mg/ml)
- NaOH (0.1 mM)

Protocol

Onto polyacrylamide (PA) gels

1. Aspirate gels thoroughly.
2. Place 20 μ l sulfo-SANPAH (100 mM) in a tube and dilute to 2 ml with HEPES (50 mM, pH 7.4).
3. Add 100 μ l of the diluted solution to each gel.
4. Immediately expose the gels to UV light for 8 minutes.

The gels should become slightly darker after this treatment

5. Wash the gels with 50 mM HEPES (pH 7.4).
6. Aspirate the gels thoroughly.
7. Repeat the previous 4 steps.
8. Prepare the collagen type I coating by gently mixing 870 μ l PBS with 100 μ l collagen type I (5 mg/ml).
9. Add 30 μ l NaOH (0.1 mM) to the coating solution and mix well.
10. Place 100 μ l of the collagen type I solution on top of every gel.
11. Incubate overnight at 4°C.

12. Wash the gels by adding 1 ml PBS to the well.
13. Remove the PBS and repeat the washing procedure.
14. Store the gels in PBS with 250 μ l Antibiotic antimycotic solution at 4°C until use.

Onto plastic substrate

1. Add 1 ml milliQ water to the well for 5 minutes.
2. Mix 50 ml PBS with 250 μ l glutaraldehyde.
3. Remove the milliQ water from each well.
4. Add 1 ml of the glutaraldehyde solution (0.5%) for 30 minutes.
5. Remove the glutaraldehyde solution (0.5%) and rinse with milliQ water.
6. Add 1 ml milliQ water and for 5 minutes.
7. Refresh the milliQ water for another 5 minutes.
8. Let the plastic surfaces dry in the laminar flow cabinet.

9. Prepare the collagen type I coating by gently mixing 870 μ l PBS with 100 μ l collagen type I (5 mg/ml).
10. Add 30 μ l NaOH (0.1 mM) to the coating solution and mix well.
11. Place 100 μ l of the collagen type I solution on top of every plastic surface.
12. Incubate overnight at 4°C.

13. Wash the plastic surfaces by adding 1 ml PBS to the well.
14. Remove the PBS and repeat the washing procedure.
15. Store the plastic surfaces in PBS with 250 μ l antibiotic solution at 4°C until use.

A.5 Experiments with PA gel substrates

Reagents

- Phosphor Buffered Saline (PBS)
- Cell culture medium (α -MEM supplemented with 10% fetal bovine serum (FBS), 1% vitamin C, 1% L-glutamine, 0.5% fungizone, 0.25% penicillin and 0.25% streptomycin)
- MC3T3-E1 cell solution
- Vitamin D (30 μ M)

Protocol

Preparation of PA gel substrates and plastic controls

1. The PA gels are stored in PBS in the wells of a 24-well plate with antibiotic solution at 4°C until use.
2. Remove the PBS and wash the gels once with PBS.
3. Add 400 μ l MC3T3-E1 medium and incubate at 37°C and 5% CO₂ for at least one hour.

Cell seeding onto PA gel substrates and plastic controls

4. Follow the MC3T3-E1 cell passaging protocol in Appendix A.1.
5. Count the cells using Muse™ Count & Viability Kit, according to manufacturer's protocol.
6. Dilute the cell solution with MC3T3-E1 medium to obtain desired cell density.
7. Gently add 400 μ l of the new cell solution into each well.
8. To the wells with an addition of vitamin D (PCD):
 - 1) The desired concentration of vitamin D in each PCD well is 1 nM.
 - 2) The volume of the cell suspension in each well is 400 μ l.
 - 3) The initial concentration of the vitamin D stock solution is 30 mM.

$$C_{Initial} = 30 * 10^{-6} \text{ mol/L}$$

$$C_{VitD} = 10^8 \text{ mol/L}$$

$$V_{well} = 0.4 * 10^{-3} \text{ L}$$

$$V_{VitD} = x$$

$$C_{Initial} * x = C_{VitD} * V_{well}$$

$$x = \frac{C_{vitD} * V_{well}}{C_{initial}} = \frac{10^8 \text{ mol/L} * 0.5 * 10^{-3} \text{ mol/L}}{30 * 10^{-6} \text{ mol/L}} = 13.3 \mu\text{L}$$

- 4) Add 13.3 μL of the vitamin D stock solution into each PCD well.
- 5) Place the 24-well plate in the incubator system at 37°C and 5% CO_2 .

A.6 Experiments with demineralised bone substrates

Reagents

- Phosphor Buffered Saline (PBS)
- Cell culture medium (α -MEM supplemented with 10% fetal bovine serum (FBS), 1% vitamin C, 1% L-glutamine, 0.5% fungizone, 0.25% penicillin and 0.25% streptomycin)
- MC3T3-E1 cell solution

Protocol

Preparation of cow bone substrates

1. The bone pieces are stored in PBS in the wells of a 96-well plate with antibiotic solution at 4°C until use.
2. Remove the PBS and wash the bone pieces once with 500 μ l PBS in each well.
3. Add 500 μ l MC3T3-E1 medium and incubate at 37°C and 5% CO₂ for at least one hour.

Cell seeding onto cow bone substrates

4. Follow the MC3T3-E1 cell passaging protocol in Appendix A.1.
5. Count the cells using Muse™ Count & Viability Kit, according to manufacturer's protocol.
6. Dilute the cell solution with MC3T3-E1 medium to obtain desired cell density.
7. Gently add 250 μ l of the new cell solution into each well.
8. Place the 96-well plate in the incubator system at 37°C and 5% CO₂.

A.7 Isolation of RNA, DNA and proteins

Reagents

- Phosphor Buffered Saline (PBS)
- Trizol
- Chloroform
- Glycogen
- Isopropanol
- Ethanol (75%, 100%)
- Distilled water
- Sodium citrate (0.1 M)
- Guanidine hydrochloride (0.3 M)
- Sodium dodecyl sulphate (1%)

Protocol

Preparation of samples

1. Remove medium from samples.
2. Wash the samples twice with PBS.
3. Add 700 μ l/350 μ l (PA gel samples/demineralized bone samples) Trizol to each well:
 - PA gels samples: pour carefully several times the Trizol over the gels and avoid to scrape the surface.
 - Demineralized bone samples: remove the bone piece into a new well before adding the Trizol solution.
4. Pipette the solution into a new set of tube and store in -80°C until use.

Isolation of RNA

5. Thaw samples if frozen.
6. Add 140 μ l/70 μ l chloroform to each sample.
7. Shake the samples by hand for approximately 15 seconds.
8. Incubate at room temperature for 2-3 minutes.
9. Centrifuge the samples for 15 minutes at 12 000 x g and 4°C .
10. After centrifugation, remove the upper water phases and transfer to a new set of tubes.
11. The remaining organic phase contains the DNA and proteins of the samples and can be stored at -80°C until use.

12. Add 5 μ l/2.5 μ l glycogen to the samples.
13. Add 350 μ l/175 μ l isopropanol to the samples.
14. Incubate the samples for approximately 10 minutes at room temperature.
15. Centrifuge the samples for 10 minutes at 12 000 x g and 4°C.
16. After centrifugation, discard the supernatant and wash the remaining pellets with 1 ml/500 μ l 75% ethanol.
17. Mix the samples by vortexing – *at this step the samples can be frozen for later usage.*
18. Centrifuge the samples for 5 minutes at 7500 x g and 4°C.
19. Carefully remove the supernatants and leave the remaining pellets to dry for approximately 10 minutes at room temperature.
20. Dilute the pellets in 20 μ l/10 μ l distilled water.
21. Incubate the samples for 15 minutes at 57 °C before measuring total RNA levels.

Isolation of DNA

The stored samples from step 11 are here to be used.

22. Add 210 μ l/105 μ l 100% ethanol to each sample.
23. Incubate at room temperature for 2-3 minutes.
24. Centrifuge the samples for 5 minutes at 2 000 x g and 4°C.
25. After centrifugation, transfer the supernatants into a new set of tubes. The supernatants contain the proteins and will be used for further separation. Store at -80°C until use.
26. Add 1 ml/500 μ l 0.1 M sodium citrate to the remaining pellets.
27. Incubate the samples for approximately 30 minutes at room temperature.
28. After 30 minutes, centrifuge the samples for 5 minutes at 2 000 x g and 4°C.
29. Refresh the sodium citrate and repeat the incubation and centrifugation procedure.
30. Again remove the sodium citrate and dilute the remaining pellets with 1.5 ml/750 μ l 75% ethanol – *at this step the samples can be frozen for later usage.*
31. Incubate at room temperature for 10 minutes.
32. Centrifuge the samples for 5 minutes at 2 000 x g and 4°C.
33. Carefully remove the supernatants and leave the remaining pellets to dry for approximately 60 minutes at room temperature.
34. Dilute the pellets in 20 μ l/10 μ l 8 mM sodium hydroxide.
35. Centrifuge the samples for 10 minutes at 12 000 x g and 4°C.
36. Remove the supernatants and place it in a new set of tubes.
37. Incubate the samples for 15 minutes at 57 °C before measuring total DNA levels.

Isolation of proteins

The stored samples from step 25 are here to be used.

38. Add 1050 μ l/525 isopropanol to each sample.
39. Incubate at room temperature for 10 minutes.
40. Centrifuge the samples for 10 minutes at 12 000 x g and 4°C.
41. Discard the supernatants.
42. Wash the protein pellets by adding 1400 μ l/700 μ l guanidine hydrochloride in 95% alcohol and incubate for 20 minutes.
43. After incubation, centrifuge the samples for 5 minutes at 7500 x g and 4°C.
44. Discard the supernatants and repeat the washing procedure three times.
45. Add 2 ml/1 ml 100% ethanol and vortex the samples.
46. Incubate the samples for 20 minutes at room temperature.
47. Centrifuge the samples for 5 minutes at 7500 x g and 4°C.
48. Carefully remove the supernatants and leave the remaining pellets to dry for approximately 60 minutes at room temperature.
49. Dilute the pellets with 100 μ l sodium dodecyl sulphate (SDS) by gently pipette up and down.
50. To completely dilute the pellets, incubate the samples at 50°C.
51. Centrifuge the samples for 10 minutes at 10 000 x g and 4°C to discard eventual pellets.
52. Transfer the supernatants containing the proteins into a new set of tubes.
53. Store the samples at -20°C until measuring total protein levels.

A.8 Detection of bone formation markers with RT-PCR

Reagents

- oligo (dT)₁₈
- Random hexamer primer
- LightCycler® water
- Reaction buffer
- 10 mM dNTP Mix
- RiboLock RNase Inhibitor (20 u/μl)
- RevertAid M-MuLV Reverse Transcriptase (200 u/μl)
- Primers (bone sialoprotein, collagen type I, ALP, osteocalcin and osteopontin)
- Primers (housekeeping genes ymHAZ and HPRT)
- Master mix

Protocol

Production of cDNA (per reaction):

1. Thaw samples if frozen.
2. Produce the primer mix by adding 1 μl oligo (dT)₁₈ and 1 μl random hexamer primers.
3. Pipette 2 μl of the primer mix into each well on a plastic PCR plate (384-well plate).
4. Add 9 μl of the isolated RNA samples into each well and finish with a negative control of 9 μl LightCycler® water.
5. Incubate the PCR plate at 65°C for 5 minutes.
6. During the incubation, make the master mix by mixing:
 - 4 μl Reaction buffer
 - 2 μl 10 mM dNTP Mix
 - 1 μl RiboLock RNase Inhibitor
 - 2 μl RevertAid M-MuLV Reverse Transcriptase
7. After incubation, put the plate on ice and add 9 μl of the master mix to each well.
8. Cover the plate with an aluminium sheet and incubate for 5 minutes at 25°C.
9. Incubate for 1 hour at 37°C.
10. Incubate for 10 minutes at 70°C.
11. Mark the plate and store at -20°C until use.

Performance of RT-PCR (per reaction):

12. Thaw forward and reverse primers.
13. Add 0.5 μl forward primer and 0.5 μl reverse primer to a new set of tubes (one tube for each primer) and dilute with 5 μl master mix and 3 μl LightCycler[®] water.
14. Produce a standard by taking 1 μl from each sample on the 384-well plate and pipette it into one of the wells of the plate.
15. Add 40 μl LightCycler[®] water to the chosen well to produce a diluted standard.
16. Pipette 10 μl of the standard into the following well and dilute with another addition of 40 μl LightCycler[®] water.
17. Repeat this procedure until five standards with different concentration of cDNA have been produced.
18. Add 9 μl of the specific solution with forward and reverse primers to all wells containing samples.
19. Mark the plate and cover it with a plastic sheet.
20. Place the plate in the PCR instrument and analyse the gene expression of the chosen bone formation markers in the samples.

A.9 Staining with NBT/BCIP

Reagents

- 0.2 M Tris Buffer
- AP Buffer with 0.2 M NaCl and 10 mM MgCl₂
- Distilled water
- Phosphor Buffered Saline (PBS)
- Formaldehyde (4%)
- Nitro-blue tetrazolium chloride/5-bromo-4-chloro-3'-indolyphosphatase p-toluidine salt (NBT/BCIP)

Protocol

1. Make 0.2 M Tris Buffer solution:
 - Mix 2.42 gram Tris with 100 ml distilled water while mixing gently.
 - Gradually adjust the pH to 10.
2. Make AP Buffer solution:
 - Mix NaCl and MgCl₂ to obtain an end concentration of 0.2 M and 10 mM respectively.
 - Gradually adjust the pH to 7.5
3. Put the PBS in water bath (37°C) for some minutes.
4. Carefully remove the medium from the wells and wash the cells with the PBS two times.
5. Fixate the cells by adding 600 µl 4% Formaldehyde during 10 minutes.
6. Gently remove the Formaldehyde and wash the wells with 500 µl distilled water two times.
7. Wash the gels carefully with tap water during 10 minutes.
8. Carefully mix 5 ml Tris Buffer with 5 ml AP Buffer in a tube.
9. Very carefully add 100 µl of NBT/BCIP to the tube. The solution should turn yellow if it is not contaminated.
10. Place the tube in a water bath at 37°C for some minutes.
11. Add 500 µl of the staining solution to each well.
12. Incubate at 37°C for 60 minutes.
13. Check the results and incubate for another 30 minutes if necessary.
14. Remove the staining solution and wash with distilled water.
15. Leave the samples with distilled water overnight to optimize removal of unspecific staining solution.

A.10 Staining with Sirius Red F3B

Reagents

- Sirius Red F3B solution
- Acidified water (5%)
- Phosphor Buffered Saline (PBS)
- Formaldehyde (4%)
- Ethanol (100%)

Protocol

1. Make Sirius Red F3B solution:
 - Add 0.5 g of Sirius Red F3B to 500 ml saturated aqueous solution of picric acid.
2. Make acidified water:
 - Add 250 μ l acetic acid to 50 ml of tap water.
3. Put the PBS in water bath (37°C) for some minutes.
4. Carefully remove the medium from the wells and wash the cells with the PBS two times.
5. Fixate the cells by adding 600 μ l 4% Formaldehyde during 5 minutes.
6. Gently remove the Formaldehyde and wash the wells with 500 μ l distilled water two times.
7. Wash the gels carefully with tap water during 10 minutes.
8. Add 200 μ l of Sirius Red F3B to each well and allow the plate to stain in room temperature for 1 hour.
9. Add 1 ml acidified water to each well and.
10. Remove the acidified water and repeat the washing step.
11. Remove the acidified water and add 500 μ l of 100% ethanol to each well.
12. Remove the ethanol and repeat the dehydration with ethanol two times.
13. Add 200 μ l tap water and allow to incubate overnight to remove more of the non-specific staining.

A.11 Staining with Alizarin Red S

Reagents

- Alizarin Red S solution
- Ammonium hydroxide (10%)
- Phosphor Buffered Saline (PBS)
- Fixative (4% formaldehyde in PBS)

Protocol

1. Make Alizarin Red S solution:
 - Mix 2 gram Alizarin Red S with 100 ml distilled water while mixing gently.
 - Gradually adjust the pH to 4.2 using 10% ammonium hydroxide.
2. Put the PBS in water bath (37°C) for some minutes.
3. Carefully remove the medium from the wells and wash the cells with the PBS two times.
4. Fixate the cells by adding 600 µl 4% Formaldehyde during 5 minutes.
5. Gently remove the Formaldehyde and wash the wells with 500 µl distilled water two times.
6. Add 200 µl of the Alizarin Red S solution to each well and allow the plate to stain in room temperature for 2 hours.
7. Remove the Alizarin Red S solution and wash the wells with pipe water to obtain superior colours.
8. Let the plate gently shake with the help of a microplate shaker during a couple of minutes to improve the non-specific staining removal.
9. Add 200 µl tap water and incubate overnight to remove more of the non-specific staining.

A.12 Staining with Goldner's trichrome

Reagents

- Weigert's Hematoxylin
- Ponceau Acid Fuchsin
- Light green SF solution
- Acetic acid (1%)
- PBS
- Formaldehyde (4%)
- Ethanol (70%)
- Ethanol (100%)

Protocol

1. Make Weigert's Hematoxylin:
 - Mix 7 ml Weigert's Iron Hematoxylin A with 7 ml Weigert's Iron Hematoxylin B.
 - Stir vigorously.
2. Make Ponceau Acid Fuchsin:
 - Pour 0,6 ml acetic acid.
 - Add 0,4 g Ponceau de Fuchsin.
 - Add 0,1 g Xylidin.
3. Make Light green SF solution:
 - Add 0,2-0,3 g Light green stock to 0,2 ml acetic acid.
 - Dilute in 100 ml distilled water.
4. Put the PBS in water bath (37°C) for some minutes.
5. Carefully remove the medium from the wells and wash the cells with the PBS two times.
6. Fixate the cells by adding 600 µl 4% Formaldehyde during 5 minutes.
7. Gently remove the Formaldehyde and wash the samples with 500 µl distilled water two times.
8. Wash the samples carefully with tap water during 10 minutes.
9. Add 500 µl Weigert's Hematoxylin to each sample and allow the plate to stain in room temperature for 15 minutes.
10. Remove the Weigert's Hematoxylin and wash the samples with distilled water.
11. Incubate with tap water for 15 minutes.
12. Repeat carefully the washing step with distilled water.
13. Add 500 µl Ponceau Acid Fuchsin to each sample and allow the plate to stain in room temperature for 15 minutes.

14. Wash the samples twice with acetic acid.
15. Add 500 μ l Light green SF solution to each sample and allow the plate to stain in room temperature for 10-15 minutes.
16. Add acetic acid to each sample for 2-4 minutes.
17. Wash the samples with distilled water.
18. Wash the samples with ethanol (70%).
19. Wash the samples with ethanol (100%).

